UNIVERSITÀ DEGLI STUDI
DI MILANO
FACOLTÀ DI MEDICINA E CHIRURGIA

FACOLTA' DI MEDICINA E CHIRURGIA

SCUOLA DI DOTTORATO IN
SCIENZE BIOCHIMICHE, NUTRIZIONALI E METABOLICHE

DOTTORATO DI RICERCA IN
FISIOPATOLOGIA, FARMACOLOGIA, CLINICA E TERAPIA DELLE MALATTIE METABOLICHE
XXVIII CICLO
Settori Scientifico-Disciplinari BIO/14-Farmacologia, MED/27-Neurochirurgia

Acquired alterations of sphingosine-1-phosphate metabolism confer stemness and drug resistance properties on glioblastoma multiforme: a new potential target for a combined approach to treat brain cancer

Giovanni Marfia
Matricola n. R10386

Docente guida: Prof. Alfredo Gorio
Coordinatore del Dottorato: Prof. Alfredo Gorio

Anno accademico 2015-2016

TABLE OF CONTENTS

ABBREVIATIONS

ABC ATP-binding cassette

bFGF Basic fibroblast growth factor

Cer Ceramide

CSCs Cancer Stem Cells

DMEM Dulbecco's Modified Eagle's Medium

DHSph Dihydrosphingosine

EGF Epidermal growth factor

GAPDH Glyceraldehyde 3-phosphate dehydrogenase

GBM Glioblastoma multiforme

GlcCer Glucosylceramide

GSCs Glioblastoma stem cells

HGG High Grade Glioma

LacCer Lactosylceramide

LGG Low Grade Glioma

MGMT O6-methyl-guanine DNA methyl-transferase

SK Sphingosine kinase

SKI Sphingosine kinase inhibitor

SM Sphingomyelin

Sph Sphingosine

S1P Sphingosine-1-phosphate

TMZ Temozolomide

FIGURES INDEX

TABLE INDEX

SUMMARY

The eradication of glioblastoma multiforme (GBM) (WHO grade 4) remains a tremendous clinical challenge in human oncology. Indeed, this tumor accounts for the most common, aggressive and lethal primary brain cancer in adults, exhibiting a dismal prognosis, despite extensive surgical resection and adjuvant radio- and chemo-therapy. The finding that GBM contains functional subsets of cells with stem-like properties named glioblastoma stem cells (GSCs) has opened up novel opportunities and promises for the development of new therapies for this devastating cancer. GSCs are self-renewing, multipotent cells, with the capacity to establish and maintain glioma tumors at the clonal level, leading to the hypothesis that they are tumor-initiating cells. Moreover, these rare subpopulations of cells possess an elevated proliferative potential, and intrinsic resistance to therapy, being thus considered a key determinant driving tumor growth, and relapse after resection and therapy. In serum free culture conditions, GSCs form neurospheres. free-floating cell aggregates with a spheroid morphology. These neurospheres preserve many of the important characteristics of the parent tumor, as cell heterogeneity and the ability to drive the parent tumor's cell invasiveness, when transplanted in murine brain. In addition, GSCs possess the capacities to give rise to a heterogeneous population of cells such as endothelial cells (glioblastoma endothelial cells, GECs) which may directly participate in the vascularization, a critical step in tumors, particularly in malignant GBM, one of the most vascularized/angiogenic tumor described. Moreover, it has been observed that microvasculature structures are the regions responsible for the localization and the maintenance of GSCs.

Different molecules, including lipid mediators appear to play a key role in the

GBM microenvironment. Among lipid mediators involved in GSC properties, ceramide (Cer) and sphingosine-1-phosphate (S1P) has recently emerged as key signals, able to control growth, invasion, and therapy resistance in various human cancers, including GBMs. Of relevance, the presence of S1P in both glioma cell lines and human gliomas is critical for tumor cell proliferation and survival, a down-regulation of sphingosine kinase 1 (SK1) suppressed growth of human GBM cells and xenografts, and a higher expression of S1P receptor 1 (S1PR1) in GBM has been correlated with poor prognosis. However, little is known on the role of Cer and S1P in GSCs. Recent studies reported that S1P acts as an invasive signal in GSCs, and that the inhibition of SKs, or the administration of a S1PR antagonist, results in GSC death. Very recently it was reported that GSCs derived from U87GBM cells, and those isolated from a human GBM specimen can release S1P extracellularly, and that S1P acts as a first messenger to enhance GSC chemoresistance to Temozolomide.

In GSC invasiveness and chemoresistance very little is known about autocrine machinery controlling GSC proliferation and particularly on the significance of S1P in these events. In order to expand previous investigation on S1P and to better understand its role on GSC activity and chemoresistance in this project I focused on the pivotal role of S1P on GSC stemness properties.

INTRODUCTION

1. Tumor of the Central Nervous System

Different benign and malignant types of tumors, have been identified in the central nervous system (CNS). The prognoses for these tumors are related to several factors, such as the age of the patient, the location, the histology, the genetic, and the microenvironment of the tumor. In adults, about half of all CNS tumors are malignant, whereas in paediatric patients, more than 75%. Neurosurgeons can offer curative resections or at least provide significant relief from mass effect for benign CNS tumors that require treatments, unfortunately, effective treatments for most malignant CNS tumors still lack. Nevertheless, the past decade has witnessed an explosion in the understanding of the early molecular events in malignant CNS tumors, and new clinical trials has been developed to target these molecular events (Adamson, Rasheed et al. 2010).

New evidence proposes that the growth of different types of cancer may be due to a subset of cancer cells which are responsible for resistance to therapy (Jordan CT, et al. 2006), and that have a significant expansion capacity to generate new tumors in relation to the neoplastic microenvironment (Reya T, et al. 2001). Moreover, within a solid tumor, in the bulk of cancer cells there are progeny of cancer stem cells, which can form new tumors and might represent a mix of partially differentiated cancer progenitor-like cells with limited proliferative capacity and terminally differentiated cancer cells, as cell with self-renewal capacity and transdifferentiating potential (Figure 1).

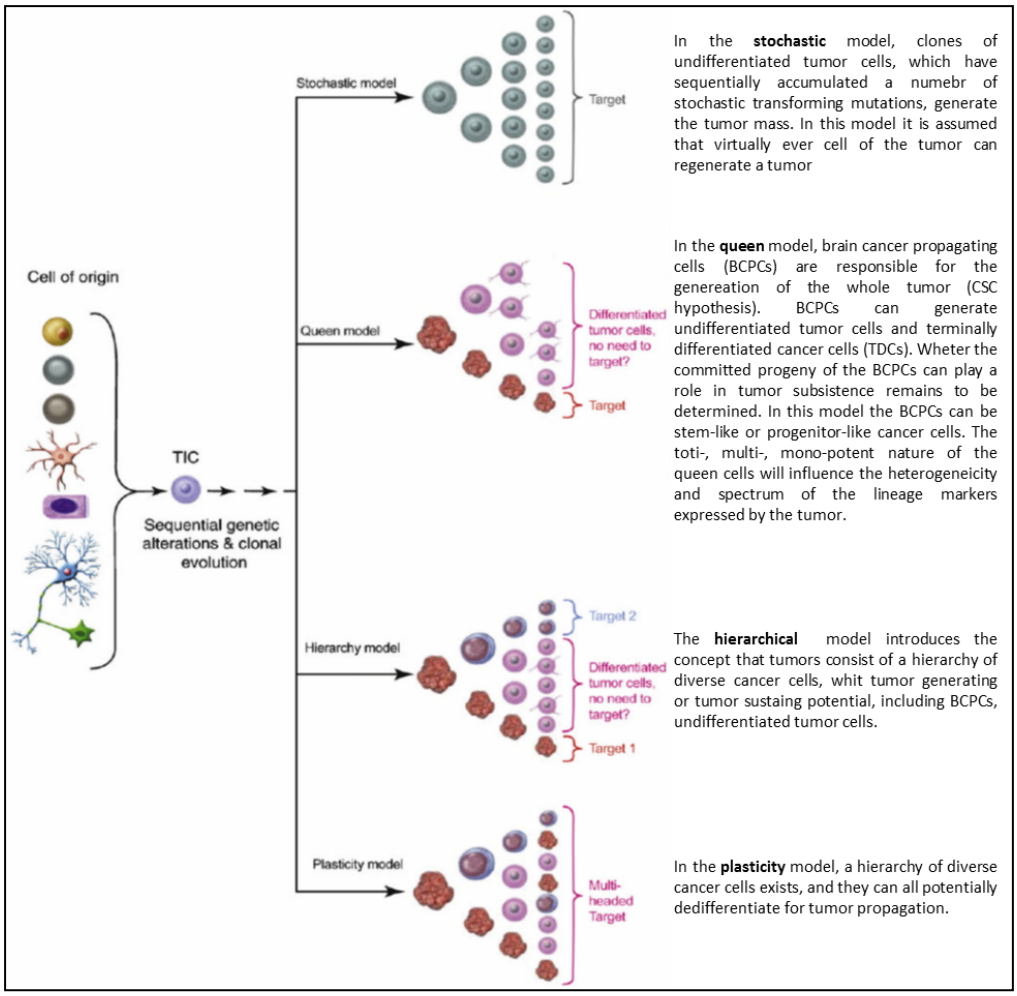

FIGURE 1: Different models of tumor formation and therapeutic targeting. Several healthy CNS cells can be potentially transformed in tumor initiating-cells (TICs) and drive the tumor growth by genetic and/or epigenetic modifications, probably due to the single cell biology and/or "neoplastic microenvironment". Various models are proposed on how these transformed cells can propagate and generate the tumor mass. No single model needs to apply to all tumor types, different models may apply to different tumor types or stages of malignant progression. (Adapted from Hadjipanayis & Van Meir, 2009).

Gliomas, so called because they arise from glial cells, are the most common primary brain tumours and an important cause of mental impairment and death (Wen PY & Kesari S, 2008). Glioma present some particular features that differentiate them from all the other CNS tumours. First, the distinction between benign and malignant lesions is less apparent than in other locations. Some glial

tumours with benign histological features, such as low mitotic index, cell uniformity and slow growth, can infiltrate entire regions of the brain, showing a clinically malignant behaviour. In addition, the anatomical location of the tumour can have fatal consequences regardless of histological features, for instance brain compression caused by an expanding tumour, resulting in severe neurological impairment.

The World Health Organization (WHO), has provided numerous grading systems to differentiate gliomas. The most common is grading system that distinguishes four different grades of gliomas based on the pathologic evaluation of the tumor. Rendering to this grading system, tumours are classified from I: least advanced disease with best prognosis, to IV: most advanced disease with worst prognosis.

Moreover gliomas are classified as: i) Low-grade gliomas (LGGs), WHO grade II, are well-differentiated (not anaplastic); these are not benign but still indicate a better prognosis for the patient; ii) High-grade gliomas (HGGs), WHO grade III-IV, gliomas are undifferentiated or anaplastic; these are malignant and carry a worse prognosis (Louis, Ohgaki et al. 2007). Grade I tumors are biologically benign and can be cured if surgically resected. Grade II tumors, as oligodendrogliomas are LGG that may follow long clinical courses, but early diffuse, and infiltration of the surrounding brain renders them incurable by surgery. Grade III tumors, as anaplastic oligodendrogliomas or astrocytomas, exhibit increased anaplasia and proliferation over grade II tumours and are more rapidly fatal. Grade IV tumours, as anaplastic astrocytoma and glioblastoma (GBM), exhibit more advanced features of malignancy, including vascular proliferation and necrosis, and as they are recalcitrant to radio- and chemo-

therapy, they are generally lethal within 15 month. Furthermore, even the most malignant, GBM rarely metastasize outside of the CNS (Buckner JC, et al, 2007).

2. Glioblastoma Multiforme

Glioblastoma multiforme (GBM) is the most common and aggressive human primary intracranial. It is the most common among gliomas with 54.7%, representing 15.7% of all CNS tumors, and 45.6% of malignant (WHO grade III and IV). The GBM is by only about 1% of adult malignancies, has an incidence of 3.19 per 100,000 and a different distribution in both sexes with a male/female ratio of 1.6/1. Predominantly it affects patients between 65 and 85 years, with a mean age at diagnosis of 64 years (Dolecek TA, et al., 2012). In most cases, GBM is a tumor of adult age, as in the group under 14 years is 0.2%, with an incidence rate of 0.14. The age of the tumor onset appears to be an important prognostic factor: several studies have shown a significant association between age and poor prognosis. Sex, however, seems to have no meaning in terms of outcomes (Walid MS.2008).

The GBM is burdened with one of the worst survival rates of all cancers in men, with a median that settles currently 14.6 months (Stupp et al., 2005). Survival rates relative, by age, are shown in Table 1.

Histologically GBM is characterized by high cellularity and mitotic activity, vascular proliferation and necrosis. Because the cells of this cancer vary in size and shape (ie are pleomorphic), the term multiforme has been previously proposed. The GBM is characterized by uncontrolled proliferation, diffuse

infiltration of adjacent tissues, massive angiogenesis, high genomic instability, and apoptosis resistance to chemo-radiotherapy, features that are useful prognostic factors for overall survival.

GBMs contain a subset of cells with characteristics of stem cell, called glioblastoma stem cells (GSCs) (Ignatova et al., 2002; Singh et al., 2004). The GSCs are self-renewing, multipotent, with the ability to establish and maintain the glial tumors and are therefore defined tumor-initiating cells (Bao et al., 2006; Lathia et al., 2011). In addition, they possess a high proliferative potential and intrinsic resistance to therapy, and may be considered as the determinant of tumor growth and the occurrence of relapses (Hadjipanayis and Van Meir, 2009).

GBMs can be divided into primary GBM (GBM or de novo) and secondary GBM (Rich & Bigner, 2004). Primary tumors comprise approximately 90% of GBM cases and are diagnosed without clinical or histological evidence of a previous low-grade neoplasia. They grow very quickly in older patients between 60 and 70 years and are characterized by a brief medical history (two-thirds of patients, less than 3 months). The secondary GBMs represent the minority of cases (<10%), derived from a low-grade tumor that undergoes a process of progression to high grade tumor. The median time to progression from a LGG to GBM is 5.3 years, from anaplastic astrocytoma to GBM is 1.4 years. The secondary GBMs typically occur in younger adult subjects with a mean age at diagnosis of 45 years and the time of progression from low to high grade ranges from months to decades (Ohgaki & Kleihues., 2007; 2009).

An additional analysis using a robust gene expression-based molecular classification obtained on 200 primary GBMs has recognized four distinctive GBM subtypes: i) Proneural, ii) Neural, iii) Classical, and iv) Mesenchymal. Aberrations and gene expression of epidermal growth factor receptor (EGFR), neurofilament 1 (NF1), and platelet derived growth factor receptor alpha (PDGFRA)/isocitrate dehydrogenase 1 (IDH1) each define Classical, Mesenchymal, and Proneural phenotype respectively. Significant similarities, but not an entirely overlap, were found between the mesenchymal and proneural phenotype. An association was observed between the Proneural subtype and age and a trend towards longer survival. Furthermore, the data suggested that Proneural samples did not have a survival advantage from the aggressive treatment protocols introduced. Importantly, an evident treatment effect was observed in the Classical and Mesenchymal subtypes (Verhaak et al., 2010).

TABLE 1. Survival rates related to age for GBM patients.

Age range	1 year	2 years	5 years	10 years
0-19	56.0	32.6	18.2	12.6
20-44	67.2	36.8	17.6	10.0
45-54	54.1	22.2	6.5	3.1
55-64	42.3	15.1	4.1	1.5
65-74	25.3	8.3	2.0	0.8
75+	10.6	3.1	0.9	-

2.1 Glioblastoma molecular markers

The characterization of malignant tumors, often takes place through molecular analysis and detection of cancer biomarkers. In oncology, they are two classes: prognostic and predictive. The firsts indicate the possible outcome of the disease, independently of the treatment received; conversely, the predictive inform about the expected outcome after application of treatment protocols. Therefore, the predictive markers help in choosing between two or more treatment options and are important for personalized therapy (targeted therapy).

Currently the widely used molecular markers to characterized GBM, evaluated in the clinical routine of brain tumors are the following: mutations of isocitrate dehydrogenase 1 and 2 (IDH1/2) gene, the methylation status of promoter of the MGMT gene, and the co-deletion of chromosomes 1p and 19q,

2.1.1 IDH mutations

Among molecular markers, IDH1 and IDH2 genotype are considered a valuable diagnostic and prognostic marker, since specific genetic mutations of these genes are able to affect the epigenetic profile of GBM. IDH1 and IDH2 are isoenzymes that convert isocitrate to α-ketoglutarate (α-KG) outside and inside the Krebs cycle, generating reduced NADPH from $NADP^+$. IDH1 functions in the cytosol and peroxisomes, while IDH2 in the mitochondria. Although both IDH1 and IDH2 mutations are described in grade II and III gliomas and in secondary GBM, IDH1 appears mostly involved in GBM compared to IDH2. Considering the histotype, IDH1 mutations are found in 50-80% of astrocytomas, oligodendrogliomas and oligoastrocytomas, while they are very rare in primary GBMs, encountered in roughly 3%, overall (vonDeimling A, et

al., 2011). Interestingly, in diffuse gliomas IDH1 mutations are strongly associated with TP53 mutations, considered driver mutations, suggesting that also IDH1 mutations may represent an early event in gliomagenesis (Ogura R, et al., 2015). Nearly 100% of IDH1 mutations are substitutions at codon 132 (Ogura R, et al., 2015). Initially, it was postulated that mutations in IDHs could abrogate the function of the encoded proteins, leading to a reduced synthesis of the α-KG metabolite. Striking new pieces of evidence have recently shown that the mutations compromise the affinity of the enzyme for the substrate and the formation of the product, resulting in increased levels of hypoxic inducible factor 1 α (HIF-1α), which facilitates tumor growth (Bolduc et al., 1995; Yan et al., 2009).

2.1.2 MGMT methylation

DNA methylation is an epigenetic modification consisting in adding a methyl group to cytosine or guanine nucleotides. Cytosine and guanine separated by a phosphate group are defined CpG islands, and are localized in the promoter region of about half of all human genes (Suzuki et al., 2009). DNA methylation at the hands of the family of methyltransferase enzymes, primarily occur in the CpG island and is associated with inactivation of transcription.

The MGMT gene located on chromosome 10q26 encoding for an enzyme involved in DNA repair, which removes alkyl groups from guanine (Pegg, 2000). The action of MGMT protects normal cells from carcinogens, but also repairs by lethal damage induced by alkylating chemotherapy, such as Temozolomide (TMZ). Methylation of the MGMT promoter is found in 35-45% of high-grade gliomas (HHG) and in 80% of low grade glioma (LGG) (Hegi et

al., 2005). Many clinical studies have shown that MGMT methylation is an independent prognostic factor associated with increased disease-free survival and overall survival of HHG, but not predictive of the sensitivity of the tumor to chemotherapy with TMZ (Gilbert et al., 2013). However, this is true for HGG patients whit tumor with IDH1 wild-type, where MGMT methylation is a predictive marker (Wick et al., 2013).

2.1.3 Loss of heterozygosity (LOH)

The most frequent genetic alteration in primary GBMs (up to 80%) is the loss of heterozygosity (loss of heterozygosity, LOH) of chromosome 10, often due to the loss of the allele (Ohgaki et al., 2004). LOH of chromosome 10 is also found up to 70% of secondary GBM, but in this case is generally partial. The chromosome 10 contains Phosphatase and tensin homolog (PTEN) and other tumor suppressor genes, which are therefore implicated in the pathogenesis of the tumor (Ichimura et al., 1998).

Also LOH for 13q and 22q are seen in primary GBM (12% and 41%) and secondary (38% and 82%) (Nakamura et al., 2005), with involvement of the loci of pRb and of the tissue inhibitors of metalloproteinases, TIMPs.

The LOH on chromosomes 1p and 19q is the most common abnormality found in oligodendrogliomas (Ohgaki et al., 2004), and the co-deletion is associated with increased chemosensitivity (Jenkin et al., 2006). Although LOH 1p is rare in primary GBMs (12%) and secondary (15%), it is associated with a higher survival. 19q LOH is more frequent in secondary GBM (54%), but rare in primary (6%) (Nakamura et al., 2000; Homma et al., 2006).

2.2 Glioblastoma treatment

Glioblastoma tumors is one of the most aggressive and difficult to treat. It grows very quickly showing high resistance to apoptosis, after radio- and chemotherapy. Moreover, the spread of drugs in the intracranial compartment is complicated by the presence of the blood-brain barrier (BBB). The standard treatment of malignant gliomas involves surgical resection, when possible, radiation therapy and chemotherapy (Stupp et al., 2008). However, the prognosis for GBM is poor, and the survival rate at 2 years is less than 15% (Wen et al., 2008; Rich et al., 2004).

Due to their infiltrative nature, malignant gliomas cannot be completely removed by surgery, but resection must be maximal, as far as possible. Cytoreductive surgical treatment (debulking) reduces symptoms caused by mass effect and provides the fabric needed to histological diagnosis and molecular studies. Advanced techniques such as image-guided neuronavigation resonance imaging, magnetic resonance imaging (MRI), and intraoperative functional mapping or intraoperative fluorescence-guided surgery, have improved the safety of surgery and increased the extent of resection that can be obtained (Asthagiri et al., 2007; Stummer et al., 2006).

Historically, radiation therapy (RT) has been the pillar of medical treatment of malignant gliomas (Walker et al., 1978). The addition of radiation therapy to surgery increased survival of patients with glioblastoma from 3-4 months to 7-12 months. It has been shown that doses less than 45 Gy determined a 13 weeks median survival compared to 42 weeks with a dose 60 Gy (Barker et al., 1996). Therefore, nowadays, standard treatment involves the administration total of 60

Gy in 30-35 fractions of 1.8-2.0 Gy, 5 days a week. The response of GBM radiotherapy is different: in many cases it can induce a remission phase with stability or regression of the neurological symptoms and decrease the size of the mass of the absorbing contrast even if the tumor typically can occur within 1 year, with neurological decline and expansion of the region absorbing contrast imaging.

The addition of chemotherapeutic agents was then shown to increase the effectiveness of RT, albeit with a modest increase in survival (6-10% on the survival rate at 1 year) (Done et al., 1993; Stewart , 2002). Despite the optimal regimen of chemotherapy (CHT) was not yet completely defined, several studies showed that more than 25% of patients received a significant benefit in terms of survival, from adjuvant CHT.

In recent years, Stupp et al, reporting the results of a randomized trial, reported that the combination of RT and TMZ, an oral alkylating agent with good penetration of the BBB, showed an increase in median survival compared to RT alone (14.6 months vs. 12.1 months) (Stupp et al., 2005). The survival rate at 2 years among patients receiving RT and TMZ is significantly higher than that of patients with RT alone (26.5% vs 10.4%), establishing RT with concomitant TMZ, the better combination for newly diagnosed GBMs (Table 2).

The recurrence in glioblastomas is however very frequent. The median time to recurrence of the disease after standard therapy was 6.9 months (Stupp et al., 2005). It strictly depends on the nature of the infiltrative tumor, which does not allow the complete elimination of malignant cells, despite the gross-total resection. Up to 90% of recurrences occur within 2.3 cm from the primary

tumor, and only 5% of patients have multiple lesions. These pieces of evidence support the thesis that recurrences originate from cancer cells that have not been removed as result of previous treatments (Choucair et al., 1986; Gaspar et al., 1992) and that have been sensitized and more resistan by RT and CHT therapies.

Nowadays, GBM therapy considers surgery, chemotherapy and biological and experimental therapies (Wernicke et al., 2011). RT for recurrence is controversial, although some studies have suggested benefits with stereotactic RT or fractionated stereotactic re-radiation. The median survival after resection of the recurrence is 3.5 months to 1 year (Nieder, et al., 2000).

TABLE 2: Gold Standard Treatment for Glioblastoma

Treatment	
Preoperative	High-dose corticosteroids, dexamethasone 8-16 mg / day. Any AED therapy (lamotrigine, levetiracetam, pregabalin).
Surgery	Resection ceiling.
Radiotherapy (RT)	Conformational fractionated in 30-35 daily doses of 1.8-2 Gy, 5 days a week, for a total of 60 Gy.
Chemotherapy (CHT)	Concomitant TMZ, 75 mg / m2 / day po on days 1-42, typically 1-1,5h before RT. TMZ adjuvant at high doses, 150-200 mg / m^2 / day po on days 1-5 every 28 days for 6 cycles.

2.2.1 Antineoplastic agents.

- Temozolomide (TMZ) is an oral alkylating agent used for newly diagnosed GBM. TMZ administration and adjuvant concomitant radiation therapy is associated with a significant increase in disease-free survival (progression-free survival, PFS) compared with RT alone (6.9 vs. 5 months), overall survival (overall survival, OS) (14.6 vs 12.1 months), and the probability of survival at 2 years (26% vs 10%). MGMT is an enzyme involved in DNA repair, which contributes to TMZ resistance. The methylation of the promoter of MGMT gene, found in about 45% of GBMs, determines an epigenetic silencing of the gene and reduces the ability of GBM cells to repair the damage, increasing susceptibility to TMZ. After TMZ treatment, patients with and without methylation have a median survival of 21.7 vs. 12.7 months, and a 2-year survival rate of 46% against 13.8%, respectively.
- The biodegradable polymer impregnated with Carmustine (BCNU) (Gliadel wafer), placed in the surgical cavity created after tumoural resection, allows for delivery of the drug directly to the site of the brain tumors. Carmustine showed a modest increase in survival (13.8 vs 11.6 months), although with increased risk of leakage of cerebrospinal fluid and intracranial hypertension, edema and abnormal wound healing process.
- The Fotemustine is a nitrosourea characterized by high lipid solubility and low molecular weight that favour the passage through the BBB. The antitumor effect is related to the ability to alkylate DNA. It is indicated mainly in recurrent GBM (Beauchesne, 2012).

- The anti-angiogenic agent Bevacizumab (Avastin) is a recombinant monoclonal antibody directed against VEGF-A, causing reduction of tumor vascularization, and inhibiting the tumor growth. Bevacizumab was approved by the FDA in 2009 for GBM treatment. Administered in combination with irinotecan (CPT-11), Bevacizumab, in recurrent gliomas, improves disease-free survival at 6 months, from 21% in patients treated with TMZ alone, to 48%. Some data suggest, moreover, that the anti-angiogenic therapy improves the efficacy of RT. Retrospective and prospective studies have shown that the anti-angiogenic therapy increases the PFS in HGGs. However, the efficacy of bevacizumab in increasing overall survival, to date, is yet to be verified (Norden et al., 2009). Indeed, numerous patients were resistant to Bevacizumab treatment, probably due to the up-regulation of alternative angiogenic factors following VEGF inhibition, such as PDGF/PDGFR-b, FGF, SDF-1a, and angiopoietin-1 (Ang-1)/Tunica interna endothelial cell kinase homolog (Tie-2), or increased pericytes mobilization, endothelial cell survival factor secretion, and induction of aggressiveness of GSC invasive phenotype with host blood-vessel appropriation and gliomatosis (Reardon DA, et al., 2008).
- Other promising areas of research include combination therapies of anti-VEGF inhibitors with vaccine strategies, immune checkpoint inhibitors, and other treatment modalities, such as newer radiotherapy techniques.

2.3 Glioblastoma Cancer Stem Cells in tumor pathogenesis

Within the GBM tumor mass are recognizable different cell subpopulations; among them cancer stem cells (CSCs) were identified as responsible for tumor birth, formation, proliferation, aggressiveness, recurrence, and resistance to therapy (Nduom EK, et al., 2012). These CSCs, named glioblastoma stem cells (GSCs), has been demonstrated to share some features with the already known somatic stem cells present in different human tissues (including the brain tissue, where normally are presented neural stem cells, NSCs), including self-renewal (by symmetric and asymmetric division) and differentiation capacity, albeit aberrant. Like the common stem cells, GSCs express certain surface markers, such as membrane antigen prominina-1 (CD133). CD133 is a transmembrane protein, used to mark "side population". Initial studies delineated clear differences between CD133 positive (+) and negative (-) glioma cells, including a dramatic difference in tumor-forming capacity in xenografts (Singh SK et al., 2003), but further studies have shown that also CD133(-) stem-like cells may also be tumorigenic (Beier D, et al., 2007; Sakariassen PO, et al., 2006). More recent studies suggest a high level of plasticity within this stem-like cancer cell population, as CD133(-) cell populations can produce CD133(+) cells after generating tumors in immunodeficient nude mice (Wang J, et al., 2008). These studies suggest that CD133 is not necessarily expressed in the GSCs in gliomas and there should be more general and sensitive makers for CSCs in gliomas. Previous studies demonstrated that GSCs expressed the main brain cancer stem cell markers: the cytoskeleton protein nestin (Zhang M, et al., 2008). Nestin is an intermediate filament protein expressed in the stem/progenitor proliferating cells during the CNS developmental stages and its expression is down-regulated in

differentiated cells. It may be involved in the organization of the cytoskeleton, cell signalling and metabolism, organogenesis, and represents the proliferation, migration and multi-differentiated characteristics of multi-lineage progenitor cells (Hadjipanayis CG & Van Meir EG, 2009). Moreover in previous study He and colleagues, demonstrated that the expression level of CD90, in GBM neurospheres was significantly increased than that in three traditional GSC adherent lines (He J et al., 2010). More recently, the same authors reported that CD90(+) cells were clustered around the tumor vasculatures in HGG tissues, suggesting a potential prognostic role for CD90 in HGG and a marker for CSCs within gliomas. Indeed, CD90(+) cells reside within endothelial niche and may also play a critical role in the generation of tumor vasculatures via differentiation into endothelial cells (He J, et al., 2012). It is possible to speculate that CD90(+) cells play a pivotal role in GBM angiogenesis, as seems that thy do not are responsible for tumor stemness (Woo SR, et al., 2015). The majority of CD90(+) cells in human GBM tissues expressed CD31, CD34 and von Willebrand factor, suggesting that they were endothelial cells (Inoue A, et al., 2015).

The neovascularization significantly correlated with enhanced tumour aggressiveness, degree of tumour malignancy, and poor clinical prognosis. Active angiogenesis, in fact, acting as a crucial event in providing oxygen and nutrients to the tumour mass as well as facilitating tumor progression, in particular in GBM, the most malignant and hypervascularized brain tumor. Indeed, it has been reported an activaction of multiple pro-angiogenic signalling pathways. Evidence establish that a pivotal role for its recaclcitrant behaviour could be assigned to the reciprocal crosstalk between GSCs and their microenvironment where endothelial cells are the principal actors. The

angiogenic process is promoted by Vascular Endothelial Growth Factor (VEGF) secretion from tumor vascular niche (Figure 2). Indeed, the GBM neovascularization significantly correlated with enhanced tumour aggressiveness, degree of tumour malignancy, and poor clinical prognosis (Li Z, et al., 2009).

However, these molecules are not GSCs universal enriched markers. In fact, it has been observed that the stage-specific embryonic antigen CD15, or stage-specific embryonic antigen 1 (SSEA-1), originally identified as a surface marker of mouse embryonic stem cells, has been recently used as an alternative marker to enrich GSCs. CD15(+) cells are often also CD133(+) and, within the tumour, are able to self-renewal, show a multilineage differentiation potential and are highly tumorigenic *in vivo* (Son MJ, et al., 2009). Recent research of Kenney-Herbert and colleagues, focused on pathogenic role for CD15 in GBM, demonstrated that CD15 could not isolate a phenotypically or genetically distinct population of CSCs in GBM. Moreover, isolated CD15(+) and (-) cells were able to generate mixed populations of GSCs *in vitro* without any significant differences in term of proliferation, aggressiveness, and xenograft tumor formation (Kenney-Herbert E, et al., 2015).

As a general consideration, these papers show that a single marker cannot be considered essential to target GSCs, in agreement with the notions that CSCs are not represented by one particular phenotype and different glioma stem cell populations (based on the expression of various markers) are present in this heterogeneous tumor. Thus, a variety of markers has to be used to better identify stem cells in all tumor cases.

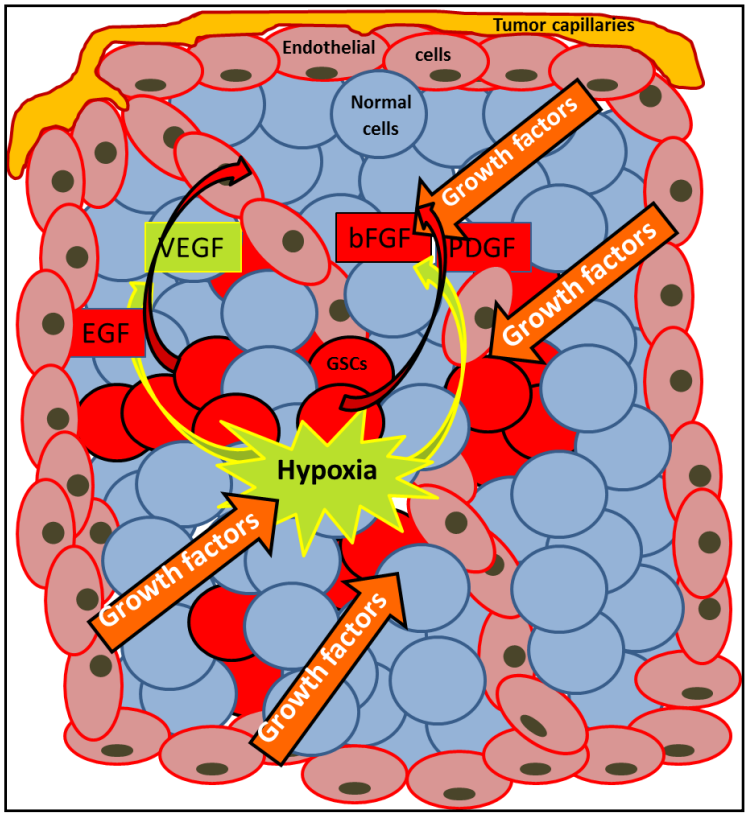

FIGURE 2: Tumor microenvironment. Regulated by oncogene activation or microenvironment conditions such as hypoxia, GSCs that reside in the perivascular niche are consistently affected by signals from tumor microenvironment, such as hypoxia, and neighboring cells (i.e. endothelial cells). In this scenario GSCs are able to secrete growth factors including pro-angiogenic factors such as VEGF that strongly stimulate angiogenesis. On the other hand, the cells of the tumor vascular compartment provide optimum conditions for the growth of GSCs.

3. Sphingolipids

In the last few years it has shown the crucial role of important metabolites, present at the level of the tumor cells and microenvironment, in determining some important characteristics such as the degree of malignancy, invasiveness, resistance to apoptosis. In this scenario, sphingolipids have emerged as crucial players. The term sphingolipids include a family of amphipathic lipids that possess functional and structural properties characterized by a hydrophilic (or

polar head) and a hydrophobic (or tail) portion. The structural element common to all sphingolipids is represented by N-acylated sphingosine, termed ceramide (Cer). They are ubiquitous as components of cell membranes (both in the plasma membrane, as in the intracellular organelles membranes), where present a polarized or asymmetric distribution and regulate the membrane fluidity and structure. Additionally, different stimuli applied to cells (such as UV radiation, chemotherapy, growth factors, etc.) generate metabolic reactions that lead to the production of different intermediate of sphingolipid metabolism, and particularly sphingosine (Sph), S1P, Cer, glucosyl-ceramide (GlcCer) and ceramide-1-phosphate (Cer1P). These molecules act as bioactive ones, and are involved, as intra- or extra-cellular messengers, in the regulation of crucial processes as cell growth, death, migration and senescence (Mignard V, et al., 2014). Although the sphingolipid family exhibits multiple diversity for structure and function, they show common biosynthetic and catabolic pathways. The center of sphingolipids metabolism is Cer that can be produced in at least three distinct ways. First, it can be originated from the *de novo* pathway, second, through the hydrolysis of complex sphingolipids (sphingomyelin and glycoshingolipids), and finally, through the recycling of fromsphingosine, derived complex sphingolipids catabolism (Adan-Gokbulut et al., 2013).

3.1 Ceramide

The backbone of the sphingolipids is the ceramide (Cer), a lipophilic molecule whose training is the first step in sphingolipid biosynthesis (Figure 3).

Cer is present in small amounts within cell membranes, as it functions primarily as an intermediate of complex sphingolipid metabolism and acts as a cell signalling mediator (Futerman AH & Hannun YA, 2004).

Cer is heterogeneous in its structure, as fatty acids with different acyl chain lengths, double bonds and hydroxylations can be present in the molecule (Merrill AH Jr, et al., 2009). Notably, this heterogeneity depends not only on the availability of different fatty acyl precursors, but mainly on the action of specific enzymes controlling the production of specific ceramide species (Park JW, et al., 2013).

Cer can be synthesized *de novo*, from the condensation of L-serine and palmitoyl-CoA, or by a route of recycling of Sphingosine (Sph), produced by the catabolism of sphingolipids. These processes occur all at the level of the endoplasmic reticulum (ER); Cer is then translocated to the level of the Golgi apparatus for the synthesis of glucosylceramide (GlcCer), ceramide 1-phosphate (Cer1P) and sphingomyelin (SM) (sphingomyelin knows also another synthetic route to the outside of the apparatus Golgi).

Recent studies have focused on the investigation of trafficking of ceramide within the cell; in particular, as mentioned above, it has identified a protein, called CERT, which mediates the transport of Cer, ATP-dependent, from the endoplasmic reticulum to the Golgi mechanism with non-vesicular mechanism (Giussani P et al., 2008). A modulation of the Cer levels in ER-Golgi compartment could be crucial for the regulation of its functions; in fact, it has been shown that the *de novo* Cer generation, its removal through the synthesis of SM and the inhibition of its transport to the site of SM synthesis are responsible for variation of Cer involved in the control of cell proliferation and in apoptosis of glioma cells (Viani P. et al., 2003).

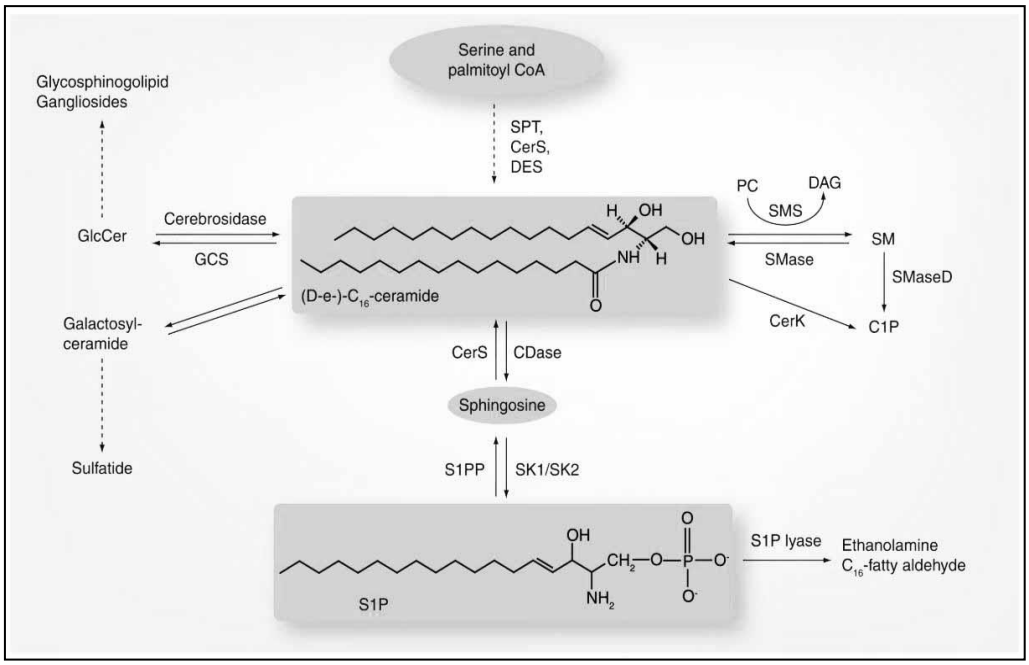

FIGURE 3: Schematic representation of ceramide and of the main related sphingolipids metabolism. SPT, serine-palmitoyl transferase; CerS, ceramide synthase; DES, dihydroceramide desaturase; GCS, glucosylceramidesynthase; GDase, glucosylceramidase; S1PP, S1P phosphatase; SK, sphingosine kinase; PC, phosphatidylcholine; DAG, diacylglycerol; SMase, spingomyelinase; SMS, sphingomyelin synthase; C1P, ceramide-1-phosphate; CerK, ceramide kinase

Among several glioma cell lines, differences with regard to the fatty acyl chain distributions of Cer were detected using liquid chromatography tandem mass spectrometry (Sullards MC, et al., 2003), suggesting heterogeneity in ceramide subfamilies in different GBMs. Of interest, a specific reduction in C18 ceramide was recently shown in human gliomas as a function of their malignancy grade, and, notwithstanding their great heterogeneity, low levels of C18 ceramide were common to different GBMs (Abuhusain HJ, et al., 2013). In head and neck squamous cell carcinoma, C18 ceramide was found to be the only form of Cer whose levels were decreased, and its levels inversely correlated with metastasis (Karahatay S, et al., 2007), suggesting that reduced C18 ceramide levels may also contribute to GBM malignancy.

3.2 Sphingosine-1-phosphate

Sphingosine-1-phospahte (S1P) is an intermediate of sphingolipid metabolism and play an important role as bioactive molecules. S1P metabolism is finely regulated through the modulation of different enzymes responsible for its synthesis and degradation (Le Stunff H, et al., 2004). S1P is formed from sphingosine (Sph) and ATP in a reaction catalyzed by two isoenzymes, sphingosine kinase 1 (SK1) and sphingosine kinase 2 (SK2) (Liu H, et al., 2002). Among all the intermediate of sphingolipids metabolism, S1P is involved in various roles like intra- or extracellular messengers for growth, death, adhesion and cell migration. With the hypothesis to demonstrate the crucial role for sphingolipids in tumor process, in my research project I focused on the S1P onco-promoter ability to act as extracellular signal, favours proliferation, stemness, angiogenesis and chemoresistance properties in GSCs.

S1P is a sphingolipid metabolite able to perform multiple tasks, and to act as powerful biomediator in various biological processes. S1P is a bioactive molecule that has antiapoptotic properties through antagonising Cer-mediated apoptosis by activating ERK and suppression of ceramide-induced JNK activation (Cuvillier, O.; et al., 1996). Moreover, previous works, performed in both cell cultures and animals, demonstrated that S1P can modulate pathological processes strictly related to cancer and inflammation, favouring cell survival, migration, and angiogenesis (Hannun YA, et al., 2008). S1P can exert its bioactive properties in the intracellular milieu, acting as a second messenger, and mainly in the extracellular milieu , where, after secretion from cells, can bind five specific cell surface receptors (S1P1-5) coupled to different G-proteins and

thereby activating several signal transduction pathways that control cell behaviour (Payne SG, et al., 2002) (Figure 4).

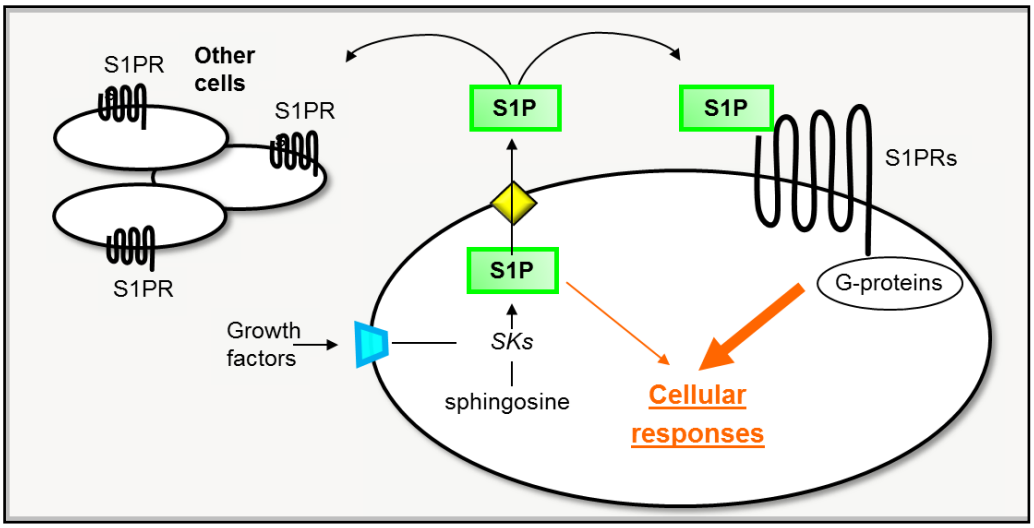

FIGURE 4: Schematic representation of sphingosine-1-phosphate roles. The bioactive properties of S1P in GBM tumor miscroenvironement is shown. SKs, sphingosine kinase; S1PR, sphingosine-1-phosphate receptor.

As mentioned above, S1P has emerged as an onco-promoter molecule. S1P is produced by the enzyme SphK, SK1 and SK2, these isoforms, together, differentially regulate cell fate, survival, migration, angiogenesis, and drug resistance, protecting cancer cells from chemotherapy-induced apoptosis, as shown on GBM cell lines and primary glioma CSCs (Riccitelli, E.; et al., 2013; Estrada-Bernal A, et al., 2006). It has been established that GBM cell lines and tissue specimens showed high expression for SK1 (Zhang H, et al., 2012), which correlates in HGG patients with worse prognosis and poor patient survival. Furthermore, the pharmacological inhibition of SK1 and SK2, or their silencing, decreased the GBM cell proliferation rate, preventing the entry into the cell cycle (Van Brocklyn JR, et al., 2009), and restores the sensitivity of GSCs to TMZ (Riccitelli E et al., 2013).

3.3 Sphingosine-1- phosphate aberrations in GBM

To reinforce their malignancy and their capacity to survive and colonize, GBMs adapt diverse 'crafty' strategies and, among them, exhibit aberrations in sphingolipid metabolism and thus altered sphingolipid levels. A key point appears to reside in the down-regulation of ceramide levels. Indeed, ceramide levels are lower in human GBM tissue compared to normal surrounding brain tissue, and the decrease in ceramide in GBMs is directly related to histological grade and patient survival (Riboni L, et al., 2002). The decrease in total ceramides with increasing glioma grade was found parallel to an increase in S1P content, ceramide and S1P levels being on average twofold lower and nine fold higher, respectively in GBM tissues than in normal gray matter (Abuhusain HJ, et al., 2013). In addition, human GBM specimens and tumor cells have markedly lower levels of sphingomyelin than non-tumor cells and normal brain, respectively (Campanella R, 1992; Barceló-Coblijn G, et al., 2011), and a recent report showed that, besides low ceramide, decreased sphingomyelin levels are associated with the GBM tumorigenic transformation (Terés S, et al., 2012). Recent studied provided evidence about possible molecular explanations responsible for the aberrant levels of ceramide and S1P in GBMs. Indeed, acid ceramidase (A-ceramidase), which converts ceramide to sphingosine, was found to be significantly up-regulated in GBM specimens (Abuhusain HJ, et al., 2013). Moreover, Jensen et al. (Jensen SA, et al., 2014) showed that B-cell lymphoma 2-like 13 (Bcl2L13), an atypical member of the Bcl-2 family overexpressed in GBM, acts as ceramide synthase (CerS) inhibitor.

Interestingly, through its binding to, and inhibiting CerS2 and CerS6 activity, Bcl2L13 functions as an anti-apoptotic protein by protecting the mitochondrial

membrane integrity. With regard to the increased level of S1P, a likely explanation should reside in the high expression of both SphK1 and SphK2 in GBMs (Van Brocklyn JR, et al., 2005; Li J, et al., 2008; Quint K, et al., 2014). In addition to SphK up-regulation, it was found that the S1P phosphatase 2 (SPP2), a S1P specific phosphohydrolase localized to the endoplasmic reticulum (ER) (Ogawa C, et al., 2003), is significantly downregulated in GBM as compared to normal gray matter samples (Abuhusain HJ, et al., 2013). Of note, SPP1 expression has been shown to increase ceramide levels at the ER by the recycling of its product sphingosine (Le Stunff H, et al., 2007), suggesting that the loss of SPP2 expression in GBM not only increases S1P but also drives Cer levels down. Of relevance is also the finding that the chromosomal region containing the gene for S1P lyase is deleted in human GBMs (Steck PA, et al., 1995), most likely favouring high levels of S1P in this cancer.

Thus it emerged that GBM is equipped to down-regulate ceramide and up-regulate S1P to drive a systematic shift in sphingolipid balance which may favour aggressiveness and protection from death. In agreement, using a mathematical model to construct how sphingolipid metabolism is altered in GBM cells compared to normal astrocytes, Mora et al. (Mora R, et al., 2010) observed that a key difference is the preferential channelling of complex sphingolipids into S1P synthesis in GBM cells, whereas in normal astrocytes, sphingosine formed in the lysosomes is mainly recycled into ceramide. S1P exerts multiple roles through its five specific receptors (S1P1–5) (Rosen H & Goetzl EJ 2005), and S1P1–3 and S1P5 receptors were found in human GBM specimens (Yoshida Y, et al., 2010;). In a recent study, Quint et al. (2014) reported that the mRNAs for all these receptors are up-regulated in human GBM

specimens compared to normal brain, with increasing order of magnitude from primary, up to recurrent and secondary GBMs (Quint K, et al., 2014).

Growing evidence implicates a complex interplay between GSCs and their microenvironment in determining GSC properties and maintenance (Filatova A, et al., 2013). Very recent studies demonstrated that GSCs are equipped with an efficient molecular machinery that allows them to rapidly synthesize S1P from sphingosine, as well as to export the newly produced S1P in their microenvironment (Riccitelli E, et al., 2013; Marfia G, et al., 2014). GSCs appear to share with normal cells of the nervous system, such as neurons and astrocytes, and also human GBM cells the capability of releasing S1P in the extracellular milieu (Anelli V, et al., 2005; Anelli V, et al., 2010). Of relevance, the amount of extracellular S1P provided by GSCs was found to be markedly higher (about tenfold) than that by astrocytes and non-stem GBM cells (Riccitelli E, et al., 2013). It is worth noting that, among stem cells, the export of S1P seems specific to GSCs, as neural stem cells have been reported to be uncapable of this export (Kimura A, et al., 2007). Thus it appears that, different from neural stem cells, GSCs possess the unique ability to enrich their extracellular milieu with S1P, that in turn could act as a autocrine/paracrine signal favouring tumor progression.

As mentioned before, GBM is one of the most highly vascularized tumor in man, and its blood vessels show enhanced endothelial cell proliferation, which is a key feature of their classification in the WHO grading system. The main trigger of angiogenesis processes in GBM is hypoxia, mainly localized in the center part of the tumor, and driven primarily by VEGF, induced by hypoxia inducible factors (HIFs).

Importantly, under hypoxia SphK1 up-regulates HIF-1 in GBM cells, by stabilizing HIF-1α through the Akt pathway and preventing its proteasomal degradation (Ader I, et al., 2008). It was also shown that HIF-2α up-regulation of SphK1 in GBM cells leads to enhancement of neovascularization (Anelli V, et al., 2008), and its product S1P acts as potent mediator of angiogenesis as VEGF (Liu Y, et al., 2000), most likely through its specific receptor S1P1. Moreover, S1P is a downstream target of different pro-angiogenic growth factors such as VEGF, EGF, PDGF, bFGF and pro-angiogenic cytokines such as interleukin (IL)-6 and IL-8 leading to a positive signaling loop (Shu X, et al., 2002).

Interestingly, it was found that in GBM cells SphK1 down-regulation, but not that of SphK2, reduced extracellular S1P levels, which in turn decreased both migration and tube formation in co-cultured vascular endothelial cells (Anelli V, et al., 2010). In addition, VEGF down-regulation was unable to block the angiogenic switch triggered by GBM-derived S1P. In GBM cells S1P is able to initiate endothelial cell sprouting, which is representative of a multistep angiogenic process, and SphK1 plays an essential role in regulating paracrine angiogenesis, favouring the early sprouting response of endothelial cells by increasing both number and length of sprouts (Abuhusain HJ, et al., 2013). Notably this effect was induced by S1P released by GBM cells, and was not affected by VEGF (Abuhusain HJ, et al., 2013), suggesting that S1P signaling is required even when potent angiogenic factors such as VEGF are present.

AIM OF THE WORK

Glioblastoma multiforme (GBM), the highest grade of gliomas (World Health Organization Grade IV), is the most aggressive and malignant human brain cancers, with a short prognosis (Siegel R, et al., 2012). Indeed, despite the introduction of aggressive and multi-modal therapy with neurosurgery, radiation, and chemotherapy, current treatment regimens have modest benefits, and recurrence of GBM is nearly universal. The overall median survival time of adult patients remains as short as 12–14 months (Serwer LP et al., 2012), only 3–5 % of patients surviving more than 3 years, with a median survival of only 5–7 months with optimal therapy (Krex D, et al., 2007). Increasing evidence suggests that a subpopulation of cells within the tumour, named Glioblastoma Stem Cells (GSCs), that possess transcriptional and epigenetic programs that endow them with stemness properties (Dick JE 2008), appears crucial in both the initiation and maintenance of this tumour, and might play a fundamental role in (i) its malignant growth, (ii) in recurrence and (iii) in resistance to chemo- and radiotherapies. Although the mechanisms of GBM onset and progression remain unclear, recent advances in the understanding of the aberrations of signalling pathways associated with GBM have opened a new window in the comprehension of its aggressiveness (Charles NA, et al., 2011). Indeed, multiple oncogenic signalling aberrations are associated with GBM, and drive its aggressive behaviour. An increasing amount of evidence indicates that also alterations in sphingolipid signalling play important roles in GBM, participating in its progression and malignant properties. However, there are still several discrepancies as well as unanswered questions. Among them, little is known about the mechanisms underlying Cer and S1P dysregulation. It is also unclear

how the multiplicity of functional actions of S1P is utilized by GBM as signal enhancement for their microenvironment, and the possible molecular circuits that integrate sphingolipids with other cell-regulatory elements of GBM. Particularly it is still unclear if GSCs are able to produce and release their own S1P extracellularly, or if S1P secreted by other neighbour cells, is the responsible for the S1P mediated responses found in GSCs. Using GSC lines derived from human glioblastoma specimens with different proliferative index and stemness marker expression, we assessed the hypothesis that sphingosine-1-phosphate (S1P) affects the proliferative and stemness properties of GSCs.

On these premises, the aim of this PhD project was to investigate the ability of GSCs to produce and release S1P in the extracellular milieu, as strategy to escape pharmacological and radio-chemo-therapies. Moreover, we evaluated the possible involvement of S1P as an autocrine/paracrine factor modulating proliferation and stemness response in GSC,, favouring a pro-stemness environment. Moreover, we evaluated the possible involvement of fingolimod (FTY720), a S1P receptor agonist, approved by the FDA for the treatment of the relapsing forms of multiple sclerosis (Kappos L, et al., 2010), in modulating the resistance to Temozolomide. The overall rationale of this research was that a deeper comprehension of the mechanism of S1P secretion and action in GBM microenvironment could improve our understanding of the GSC chemo-resistance, representing a critical step to develop new GBM therapeutic compounds able to modulate S1P metabolism to curtail GBM progression.

MATERIALS METHODS

4.1 Patients and study design

This was an observational study performed on patients affected with grade IV gliomas who underwent neurosurgical procedures at the Neurosurgery Units of Fondazione IRCCS Ca' Granda Ospedale Maggiore Policlinico in the last 3 years. Demographic and clinical data were retrospectively collected from patients' files, starting from the date of diagnosis until death or the date of the last visit performed, whichever came first. Karnofski Performance Status (KPS) was assessed on the day before surgery. Written informed consent was obtained from patients or their caregivers before surgery. The study was approved by the Institutional Review Board of the hospital.

4.2 Eligibility

Patients of both sexes with newly diagnosed malignant brain tumors who signed a written informed consent were eligible for this study. Inclusion criteria were: intraoperative histologically proven diagnosis of malignant brain tumor on review by two independent pathologists; 18-80 years of age; Karnofsky performance status >60; negative human immunodeficiency virus serology; no evidence of acute or chronic hepatitis on standard hepatitis C and B screening tests; no second malignancies. Exclusion criteria were: not proven diagnosis of malignant brain tumor by the biopsy during the operation of malignant brain tumor after surgical resection; concomitant life-threatening disease; presence of acute (including respiratory) infection; positive serology for human immunodeficiency virus, hepatitis B or C; history of other malignancies; and compliance with the study protocol.

4.3 Histopathological Analyses

Histology was performed on specimens fixed in a 4% paraformaldehyde (PFA) solution (Sigma-Aldrich, Basel, Switzerland) in Dulbecco's phosphate-buffered saline (D-PBS) (Euroclone, Milan, Italy) and subsequently embedded in paraffin, cut at 30 μm, and stained with haematoxylin-eosin. GBM samples were histologically confirmed and classified as grade IV GBMs, in accordance with WHO established guidelines (Louis et al., 2007).

4.4 Immunohistochemistry

The sections were deparaffinised and then dehydrated. In the next step, blocks were incubated in fresh citrate/HCl buffer solution for antigen recovery and, after 60 min incubation, were washed with D-PBS. Samples were then incubated with biotinylated monoclonal Ki-67/MIB1 antibody (1:100; Ventana, Tucson, AZ, USA) and rabbit anti-glial fibrillary acidic protein (GFAP; 1:200, Chemicon, Temecula, CA, USA). Then the slides were exposed to peroxidase-labeled streptavidin followed by washing with D-PBS, and finally exposed to diaminobenzidine hydrochloride chromogen (BD Biosciences, San Jose, CA). Afterwards, they were covered with coverslips following dehumidification. Stained slides were observed by a pathologist using an Olympus BX41 (Olympus, Tokyo, Japan) light microscope.

One thousand tumor cells were counted in several areas of tissue where positively stained nuclei were evenly distributed. In those cases with uneven distribution of positive nuclei, the tumor cells were counted in the areas with highest density of positive nuclei by visual analysis (Ralte et al., 2001). The Ki67 labelling index was calculated as a percentage of labelled nuclei.

4.5 Loss of heterozygosity 1p and 19q

Loss of heterozygosity (LOH) of chromosome arms 1p and 19q was assessed by short tandem repeats (STR) analysis using paired tumor specimens and PBLs.

The LOH was investigated using the following STR markers: D1S468, D1S548, D1S2666, D1S1612, D19S918, D19S596, D19S206. A total of 100 ng of tumor and PBL DNA was amplified by PCR, with settings optimised individually for each primer pair. PCR products were then analysed by capillary gel electrophoresis on the GeneMapper ABI 3130XL (Applied Biosystems, Foster City, CA, USA). Criteria used to establish LOH were the same reported by Johnson et al. (Johnson MD1, et al., 2003).

4.6 Detection of IDH1 and IDH2 mutations

IDH1 codon 132 and IDH2 codon 172 mutations were screened by MassArray iPLEX platform (Agena Bioscience, Hamburg, Germany) based on matrix-assisted laser desorption ionization time-of-flight (MALDI-TOF) mass spectrometry. PCR and downstream reactions were performed according to the manufacturer's instructions. PCR and Extended primers were designed manually to detect all possible nucleotide substitutions at these positions and specific oligo tag sequences were added to the 5'end of each PCR primer to optimize the PCR reaction. PCR multiplex amplification was conducted in 5μl reaction mixture containing 30 ng of tumor DNA, 100 nM each designed primers, 100 nM dNTP mix, PCR buffer, 25 mM MgCl2, and 5U Taq DNA polymerase (Agena Bioscience, Hamburg, Germany). The mixture was incubated as follows: 95 °C for 2 minutes, 45 cycles of 95 °C for 30 seconds, 56 °C for 30 seconds, and 72 °C for 60 seconds and then a final extension step at 72 °C for 5 min. The

remaining unincorporated dNTPs were removed by the SAP treatment with 1.7 U of Shrimp Alkaline Phosphatase (SAP): the plates were incubated at 37 °C for 40 min and then at 85 °C for 5 min. Finally, the iPLEX reaction mix, including iPLEX Buffer Plus, iPLEX Termination Mix, Extended Primers mix, and iPLEX enzyme (Agena Bioscience, Hamburg, Germany), was added to the PCR amplification products. The iPLEX reaction was carried out in the following conditions: at 94 °C for 30 s; 40 cycles at 94 °C for 5 s [52 °C for 5 s and 80 °C for 5 s (repeated five times per cycle)]; and a final extension step at 72 °C for 3 min. The samples were desalted by resin treatment and spotted on a SpectroCHIP (Agena Bioscience, Hamburg, Germany). The chip was analysed by mass spectrometry. The spectrum profiles generated by MALDI-TOF-MS were acquired and examined with SpectroTYPER 4.0 software (Sequenom, Inc., San Diego, CA).

4.7 Determination of MGMT promoter methylation status

Tumor DNAs were subjected to sodium bisulphite conversion using the EZ DNA Methylation-Gold Kit (Zymo Research Corporation, Irvine, CA, USA). A total of 50–100 ng of the bisulphite-treated DNA was amplified PCR using 10pmol of forward (5'-GTTTYGGATATGTTGGGATAG-3') and reverse primers (5'-bioCRACCCAAACACTCACCAAA-3'). The PCR conditions for MGMT gene were: 95°C for 5 minutes, 45 cycles of 95°C for 30 seconds, 56°C for 30 seconds and 72°C for 20 seconds; at the end of this cycles, a final elongation step was performed at 72°C for 5 minutes. Quantitative DNA methylation analysis of 10 CpGs (CpGs 74-83) [23] was performed on the Pyro Mark ID instrument using the Pyro Gold Reagents and 1 pmol of sequencing

primer (5'-GATAGTTYGYGTTTTTAGAA-3'). Data were analyzed with the support of the Q-CpG software v1.09 (Qiagen, Hilden, Germany).

4.8 Establishment of primary cultures of GSCs

After surgical removal, tumor samples of 57 patients were placed in D-PBS supplemented with 1% penicillin/streptomycin (Sigma-Aldrich, Basel, Switzerland). GSCs were isolated essentially as previously described (Salmaggi et al., 2006, Riccitelli et al., 2013; Marfia et al.,2014), with some modifications. In particular, samples were mechanically dissociated in a Petri dish with a scalpel, and suspension was collected with D-PBS, and centrifuged (300g for 10 min). The pellet was enzymatically digested by treatment with 0.25% Liberase Blendzyme2 (Roche Diagnostics, Indianapolis, USA) in D-PBS for 4h. After dilution with D-PBS, the suspension was centrifuged as above. Cells were then resuspended in Stem Cell Medium (SCM), consisting of Dulbecco's modified Eagle's medium (DMEM)/F12 (1:1) containing 10 ng/mL fibroblast growth factor-2 (bFGF) (Peprotech Inc. Rocky Hill, NY, USA), 20 ng/mL epidermal growth factor (EGF) (R&D Systems, Minneapolis, USA), and 1% penicillin/streptomycin. Cells were then seeded in 75-cm^2 flasks, and grown in a humidified incubator containing 5% CO_2 and 5% O_2 at 37°C.

Primary cultures of GBM cells were obtained from an aliquot of the pellet obtained from tumor specimens as described above. Cells were plated in DMEM supplemented with 10% fetal bovine serum (FBS) (v/v), 2 mM L-glutamine, 100 units/mL penicillin, 100 lg/mL streptomycin, and 0.25 lg/mL amphotericin B and incubated at 37°C in 5% CO2 humidified atmosphere.

Culture medium of both GSCs and GBM cells was refreshed twice per week to

guarantee constant supply of required growth factors and nutrients. Both cell types were detached and dissociated weekly using Tryple Select (Gibco, Grand Island, NY, USA).

Cells were observed with an inverted phase-contrast microscope (Nikon Eclipse TE300, Nikon, Shinjuku, Tokyo, Japan), and images were acquired with a digital camera (Zeiss Axiovision, Zeiss, Oberkochen, Germany), using Axion Vision software (Zeiss).Cell viability was evaluated by Trypan Blue dye-exclusion assay, and cells counted in a Fuchs-Rosenthal chamber.

4.9 Selection of two lines representative of slow- and fast-proliferating GSCs

From 57 GBM tissue samples, we isolated 30 GSC lines and two of them, as representative of slow- and fast-proliferating cells were selected. The two GSC lines derived respectively from two patients (pts): pt1 (as slow proliferating cells) and pt2 (as fast proliferating cells), displaying the following features: aging 56 (pt 1), and 59 years (pt 2), and the preoperative Karnofsky performance status (KPS) was normal (100%) in pt 1, and low (60%) in pt 2.

4.10 Immunophenotypic analyses

Immunophenotypic analyses of GSCs were performed by FACS, using single cell suspensions. For each analysis, $5.0x10^4$ cells were incubated with the appropriate phycoerytrine- (PE) or fluorescein isothiocyanate- (FITC) conjugated antibody to evaluate the expression of the following pattern of stemness and endothelial progenitor markers: CD15, CD31, CD34, CD45, CD133 (Miltenyi Biotec, Bisley, Surrey, UK), and CD90 (Millipore Temecula, CA, USA). Isotype-matched mouse immunoglobulins were used as control.

After 30 min at 4° C, cells were washed once with D-PBS, centrifuged at 300g for 10 min, and finally fixed with 4% PFA. Cell analyses were performed on a FACS flow cytometer and CellQuest software (BD Biosciences, San Jose, CA). A Forward Scatter vs. Side Scatter dot plot was used to include only viable nucleated cells. Post-processing data analyses were performed with FlowJo software (Treestar, Inc. Ashland). At least $2x10^4$ events per sample were acquired.

4.11 GCS proliferation assays

GSCs were plated in 12-well multiplates (3.0×10^5 cells/well) in SCM, and incubated in 5% CO_2 and 5% O_2 at 37°C for 7 days. At the end, cells were collected and centrifuged (300g, 10 min). The supernatant was discarded, and the pellet was re-suspended in 400 μL of TrypLE Select (Gibco) and incubated at 37° C for 5 min. The suspension was then mechanically dissociated by pipetting up and down for 2 min at room temperature, then neutralized with an equal volume of SCM, and centrifuged as above. Viable cells were then counted by Trypan Blue dye-exclusion assay, using a Fuchs-Rosenthal chamber. Growth curves were obtained by counting the number of viable cells at each passage one week after plating. To evaluate the proliferation index, GSCs were plated in SCM as above, and the index was calculated by dividing the cell number at specific time points (2 and 7 days) and the number of input cells at time 0.

4.12 Cell cycle analysis

Cells ($5.0x10^5$) were fixed in one mL of cold ethanol (70% vol/vol in D-PBS) with gentle vortexing (5 sec) to obtain a mono-dispersed cell suspension, and

maintained in ethanol, at 4° C, for at least 2 h. Cells were then centrifuged (300g, 10 min) and the ethanol thoroughly decanted. The pellet was re-suspended in 500 µL of D-PBS and incubated with 10 µg/mL RNAse A, at 37° C for 15 min. After centrifugation as above, the new pellet was resuspended in 500 µL of D-PBS containing 50 µg/mL propidium iodide, and incubated at 37°C, 20 min in the dark. Cell cycle distribution was measured on a FACSCalibur flow cytometer, and data analyzed using Cell Quest software (BD Biosciences, San Jose, CA).

4.13 Intracranial xenograft studies

To assess *in vivo* tumor formation and growth, adult 6-week old NOD-SCID mice (Charles River, Calco, Lecco, Italy) were used for transplants. We minimized the number of animals used in experiments and did great efforts to reduce their sufferings. All surgical procedures were performed under sterile conditions and aseptic manner, and were performed according to NIH and institutional guidelines for animal care and handling. Animals (n=5 for each cell line) were deeply anaesthetized, and cells were injected stereotactically into the frontal lobe, essentially as we previously described (Salmaggi et al., 2006). In detail, a burr hole was made in the skull 1.2 mm lateral to the bregma using a drill, and $2.0x10^5$ cells in 2 µl of PBS were stereotactically injected over 3 min at a depth of 4 mm. At 5 weeks mice were anesthetized and transcardially perfused with 4% paraformaldehyde in saline. The brains were removed, post-fixed and prepared for histology (Salmaggi et al., 2006). Tumor volume was calculated by measuring the diameter and length of each tumor in the respective slide with the maximum tumor size (Schmidt et al., 2004). Maximal and minimal diameter of

the tumor was measured in mm on Hematoxylin and Eosin (H&E) stained sections and the approximate tumor volume was calculated using the following formula: tumor volume (mm^3) = (max. diameter) x (min. diameter)^2 x 0.5.

In order to identify human cells, slides were labeled with a specific mouse anti-human nuclei antibody (MAB 1281, Chemicon) (1:50, overnight at 4°C). Next they were washed and incubated with secondary antibody Cy-3-conjugated antimouse IgG (1:1000, Jackson, Bar Harbor, Maine, USA) for 1 h at room temperature and then washed again and counter stained with 4'-6-diamidino-2-phenylindole (DAPI) to identify cell nuclei. Immunofluorescence measurements were made using a confocal microscopy (Leica System, Wetzlar, Germany).

4.14 Metabolic Studies by Cell Labeling

Metabolic studies using [C3-3H]-D-erythro-sphingosine (3H-Sph) (PerkinElmer, Boston, MA, USA) were performed as previously reported (Riboni et al., 2000), with some modifications. In detail, at the time of experiment, cells were plated in 6-multiwell plates (5.0 x 10^5 cells/well), and incubated for a given period of time in complete SCM containing 20 nM–1μM 3H-Sph (0.4 μCi/mL) and phosphatase inhibitors (Riccitelli et al., 2013). After exposure to 3HSph for different times, GSCs were centrifuged (500g, 5 min at 4°C), and media and cells were collected. Cellular internalization of Sph was confirmed by radioactivity counting, and possible cytotoxic effects were excluded by a cell viability assay.

4.15 Sphingolipid and S1P Extraction and Purification

Total lipids were extracted from cells with chloroform/methanol at 4°C as

previously reported (Anelli et al., 2005). Briefly, after partitioning of the total lipid extract, the upper alkaline aqueous phase (containing S1P) was evaporated under a nitrogen stream and counted for radioactivity. The lower organic phase (containing Ceramide, sphingomyelin, and neutral glycosphingolipids) was subjected to a mild alkaline hydrolysis by the addition of 0.15 volumes of 0.1 M NH4OH, and the phases were then separated by centrifugation.

Extracellular S1P was extracted and partially purified from cell medium by a two-step partitioning, at first in alkaline conditions; then a back extraction of the aqueous phase was carried out in acidic conditions (Anelli et al., 2005). The final organic phase, containing extracellular S1P, was then evaporated under a nitrogen stream.

4.16 Separation and Quantification of Sph Metabolites

Sphingolipids in the methanolysed organic phase and aqueous phases were counted for radioactivity by liquid scintillation, and applied to silica gel HPTLC plates (Merck, Darmstadt, Germany). The plates were developed in chloroform/methanol/water (55:20:3, by vol.) for the organic phase. For the quantification of ^{3}H-SlP, the fractions containing cellular and extracellular S1P were applied to HPTLC plates and developed in n-butanol/acetic acid/water (3:1:1, by vol.). Standard ^{3}H-S1P, obtained from ^{3}H-Sph by enzymatic phosphorylation (Anelli et al., 2005), was chromatographed on the same plate, and used as internal standard.

At the end of the chromatographic separation, HPTLC plates were submitted to digital autoradiography (Beta-Imager 2000, Biospace, Paris, France). The radioactivity associated with individual sphingolipids was determined with the

β-Vision analysis software provided by Biospace. The recognition and identification of radioactive Cer, sphingomyelin, glucosyl-ceramide (Glc-Cer), and S1P were performed as previously reported (Anelli et al., 2005; Riboni et al., 2000). ^{3}H-S1P degradation was quantified as tritiated water in the final aqueous phase of medium partitioning. To this purpose, aliquots of the aqueous phase of the partitioned media were submitted to fractional distillation (Anelli et al., 2005), and counted for radioactivity as above.

4.17 Cell Treatments on GSCs

For S1P treatment, stock solution of S1P (100 mM) (Enzo Life Sciences, Farmingdale, NY, USA) was prepared in fatty acid free bovine serum albumin (4 mg/mL in D-PBS). For FTY720 treatment, FTY720 (Cayman Chemicals, Ann Arbor, MI, USA) was dissolved in absolute ethanol at a concentration of 5 mM. For TMZ treatment, TMZ (Schering- Plough, Segrate, Milan, Italy) was dissolved in DMSO. At the time of the experiments, stock solutions were diluted at 200nM (S1P), 100μM (TMZ) and 100nM (FTY720) final concentrations in fresh SCM and administered to cells. After incubation for 48h, the number of viable cells, the apoptotic and necrotic events, the proliferation index, and the cell cycle were analyzed.

4.18 Assessment of Apoptosis

To evaluate apoptosis, GSCs were processed by human Annexin VFITC kit (BMS306FI, Bender MedSystems, Vienna, Austria). Briefly, cells were collected, washed in cold D-PBS and resuspended in 200mL of binding buffer (10mM Hepes/NaOH, pH 7.4, 140mM NaCl, 2.5mM CaCl2) containing 5 mL of

Annexin VFITC solution. The mixture was incubated for 10 min in the dark at room temperature, and at the end, 1 mL of binding buffer was added. After washing with D-PBS, the final cell pellet was resuspended in 200 mL of binding buffer, containing 1mg/mL propidium iodide), and samples were immediately analysed by flow cytometry. This double staining procedure allowed us to distinguish early stage apoptotic cells (Annexin V1/Propidium Iodide-), from late stage apoptotic cells (Annexin V1/Propidium Iodide1), and necrotic cells (Annexin V-/Propidium Iodide1). Data were acquired by a FACS flow cytometer and analyzed by CellQuest software (BD Bioscence, San Jose, CA).

4.19 Analysis of cell viability

Cell viability was determined by MTT assay. GSCs were seeded at $2x10^4$ cells/cm^2. The day after, cells were treated with different treatments for the 48 hours. The medium was then replaced by MTT dissolved in fresh medium (0.8 mg/ml) for 4 hours. Then GSCs were incubated 10 minutes in isopropanol/formic acid (95: 5 v/v) to solubilisation of formazan crystal, and the absorbance (570nm) was measured using a microplate reader (Wallack Multilabel Counter, PerkinElmer, Boston, MA, USA).

4.20 Assessment of autophagy

Cells were grown on a chamber slid and, after different treatments, were incubated with 1µg/mL acridine orange (Sigma-Aldrich, St Louis, MO) (15 min) and then with 5µM Hoechst 33342 (Sigma-Aldrich, St Louis, MO) (15 min). The sample was mounted with ProLong® Gold Antifade Mountant (LifeTechnologies) and images were capture using a Leica TCS SP5 confocal

microscope (Leica Microsystems, Wetzlar, Germany). Cells were counted in three microscopic fields in each well (three wells per treatment) and expressed as a percentage of the total number of cells. Each treatment was performed in triplicate.

4.21 Immunoblot analysis

Cell lysates (60 μg of proteins) of GSCs were analysed by immunoblotting with anti- LC3B and anti-GAPDH antibodies. In detail, GSC lines were lysed in the presence of a complete protease inhibitors cocktail with 20mM Tris-Cl (pH 7.4), 1% Triton X-100, 100mM NaCl, 1mM EGTA, 2mM MgCl2, 5mM β-glycerol-phosphate, 2 mM Na-pyrophosphate, 2 mM Na-orthovanadate, 1 mM DTT, 1mM NaF, and 1mM PMSF. Cell proteins were resolved by SDSPAGE on 18% gels. The membranes were then blocked in 5% milk using TBS-Tween 0.1%, incubated for 1 hr at room temperature with anti-LC3B (1:1000) (Sigma, St Louis, MO), and then with horseradish peroxidase-linked secondary antibody for 30 minutes at room temperature. Bound antibody was visualized by ECL (Supersignal West Pico, Pierce Biochemicals, Rockford, IL, USA), and membranes were exposed to Kodak Biomax film.

4.22 Statistical Analyses

The data are shown as mean ± standard deviation (SD) of at least three independent experiments, performed in triplicate using separate culture preparations. The statistical significance was determined by the two-tailed Student's t test. Differences were considered statistically significant at $P<0.05$.

Moreover, continuous variables were expressed as median values and interquartile ranges (IQR), and compared by the Mann-Whitney *U*-test. Categorical variables were expressed as frequencies and percent values, and compared by the chi-squared test. Mortality rates with 95% confidence intervals (95%CI) were calculated as the number of events per 1 person-year. For the same purpose the tumor volume was categorized by choosing as cut-off the median value observed in the study population (i.e., 25 cm^3). Rho correlation coefficients were calculated by the Spearman's test. The Cox proportional hazard model was used to estimate potential risk factors of death and the effect of each variable was adjusted for the others in the multivariate model. In this model death was the event and follow-up duration was the time variable. The follow-up period for each patient was calculated starting from date of diagnosis to death or last visit at time of medical files review, whichever came first. The results were expressed as crude and adjusted hazard ratios (cHR and aHR) with 95%CI. Starting with the full model, stepwise backward elimination was used as a variable selection procedure. A nominal α level of 0.10 as a cut-off for removing variables was considered. All p values reported are two-sided and a value <0.05 was considered statistically significant. All analyses were done with SPSS software (release 21.0, IBM Corp., Armonk, New York).

RESULTS

5.1 Patients

Overall 57 patients who underwent neurosurgical procedures for GBM between February 2012 and June 2015 were included in the study. All patients underwent surgical resection of the lesion. The main characteristics of the 57 patients at study entry are reported in Table 3. Overall the median preoperative KPS was 80 (IQR: 70-90) and it was inversely correlated with age (r=-0.43, p<0.0001). In GBM patients the volume of the tumoral lesion was calculated from magnetic resonance imaging and the median tumor volume was 25.6 cm^3 (IQR: 8.0-45.3). The tumoral volume was calculated as mean of 25.8 cm^3 (IQR: 8.0-45.0).

5.2 Survival analysis in patients with Glioblastoma

A survival analysis was also performed in a subgroup of 57 patients with Glioblastoma (i.e. grade IV WHO glioma). During the follow-up 34 patients (60%) died after a median of 0.8 years (IQR: 0.4-1.4) from diagnosis with a mortality rate of 0.4 per person-year (95%CI 0.3-0.6). The main characteristics of this patient group are shown in Table 3. The genetic and epigenetic pattern of these patients was characterized by the presence of 1p/19q co-deletion in 2 patients (3%), an unmethylated status of MGMT promoter in 28 (49%) and a wild type IDH1/2 in 39 (68%).

The cumulative 1-year survival was shorter in patients with a tumor volume > 25 cm^3 (46 vs 83% in those with tumor volume < 25 cm^3; p=0.02). No difference in the survival rate was found by comparing patients with methylated and unmethylated MGMT promoter. By univariate Cox regression analysis age > 60 years at time of surgery (cHR 2.6; 95%CI 1.4-4.9), preoperative KPS < 70 (cHR

2.5; 95%CI 1.2-5.5), a tumor volume > 25 cm^3 (cHR 2.1; 95%CI 1.1-4.2) and wild type IDH1/2 (cHR 4.8; 95%CI 1.3-16.9) resulted risk factors of decreased survival. Owing to the small sample size no multivariate analysis was performed in this group.

Interesting, the tumor volume was significantly bigger in patients who died than in those who were survivors at the end of the follow-up period (median 32.5 vs 23.4 cm^3; IQR: 16.3-53.0 vs 6.4-35.0, respectively; p=0.04).

TABLE 3: Main characteristics of the GBM patients included in the study

	Patient with GBM (n=57)
Male sex (%)	41
Meadian age at the study entry, yrs (IQR)	61 (48–71)
Median follow-up duration*, yrs (IQR)	0.9 (0.4-1.5)
Patient alive at the end of follow-up (%)	30 (45)

yrs: years; IQR: interquartile range

*Follow-up duration was calculated from the date of diagnosis to date of death or last follow-up visit whichever came first.

5.3 Genomic and epigenetic results

The 1p/19q co-deletion was detected in 5% of GBM patients; while the R132H mutation of *IDH1* were found in the 15% of our patients. Also the median rate of methylation of the MGMT promoter was identified in 8% of GBM patients (IQR: 4-26).

5.4 Histological analysis and proliferative features of human GBMs

Microscopically, GBM specimens were composed of poorly differentiated glial cells, with numerous multinucleated giant cells. Confluent areas of necrosis and parenchymal destruction with serpiginous foci were present. Vascular proliferation was seen throughout the lesions, often around necrotic areas and in peripheral zones of infiltration. Diffuse reactivity for GFAP, regularly distributed, was seen in both cases. Proliferative activity was prominent, with detectable mitosis in nearly every field. Areas with large number of Ki67 stained nuclei in brown, reflecting active cellular proliferation, (Fig. 5A). The mean value of Ki67 labeling index, determined by the Ki-67antibody, was 34±10 %.

We isolated with a success rate of 52.6%, 30 GSC lines from 57 initial GBM specimens. We characterized cells for stemness, growth capability, tumorigenic potential, and surface marker expression.

5.5 Selection of two GSC lines, as representative of two group with different proliferation rate.

We investigated the proliferation behavior of our GSC lines. As shown in figure 5B, we evaluated for each GSC line the number of viable cells at each passage, defining their proliferation capacity.

About the proliferation rate we noticed that our cell lines behaved fundamentally in two different ways, so we decided to separate GSC lines into two groups: i) slow proliferating group and ii) fast proliferating group (Figure 5B) .

Following our hypothesis that S1P and its metabolism play a crucial role in GBM aggressiveness, favoring the proliferation of GSCs and sustaining the tumor microenvironment, we selected two GSC lines as representative of the

two distinct groups. GSCs obtained from slow proliferating group was called SC01 and the other, selected among fast proliferation GSC lines was called SC02.

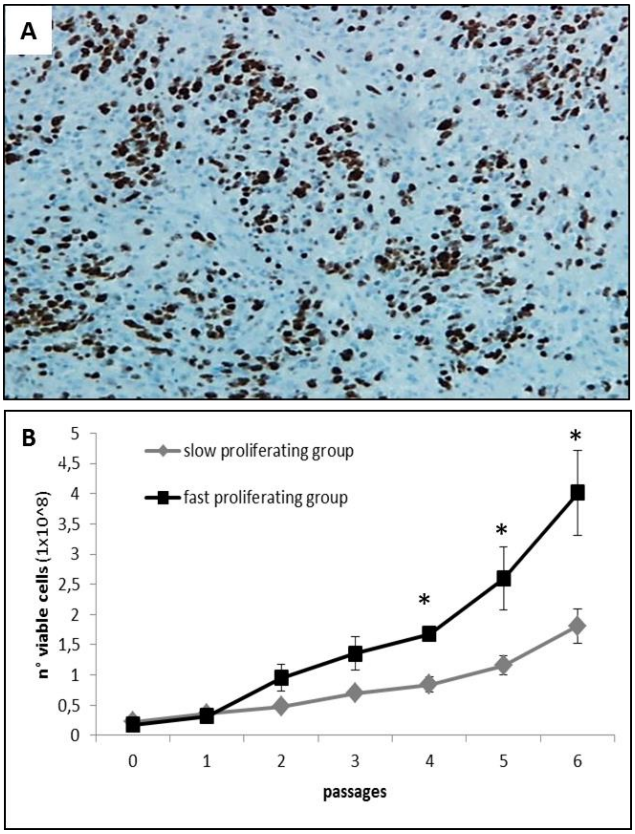

FIGURE 5: Ki-67 immunoreactivity of GBMs and GSC growth curves. A: Tumor tissue from SC02 stained with anti-Ki-67 antibody. The image shows positive nuclear expression of Ki-67 in brown and negative nuclei counterstained in blue (magnification, 40x). B: the graphic illustrate growth curves of slow- and fast-proliferating groups, showing the number of viable cells at each passages.

5.6 SC01 and SC02 grow as neurospheres and exhibit in vivo tumorigenic potential

In appropriate culture conditions that favor GSC survival and proliferation, GBM-derived cancer cell lines from slow- and fast-proliferating groups formed GSCs that grew as free floating clusters, namely neurospheres (Figure 6A and 6B, respectively). GSCs were next validated *in vivo* for their tumorigenic

potential in immunodeficient mice. After intracranial injection, both GSC lines formed tumors in all injected mice (Figure 6C). The mean tumor volume ± SD at sacrifice was 9.1 ± 4.8 mm^3 and 12.9 ± 5.5 mm^3 in SC01 and SC02, respectively (Figure 6D).

The human origin of the tumor was demonstrated by the positive staining with an anti-human nuclei antibody, which identified cells positive to human marker in the slides (Salmaggi et al., 2006). These results, showing that both cell lines exhibit the capacity for sphere formation, and are tumorigenic in brains of immunocompromised mice, demonstrated that SC01 and SC02 expressed functional features of GSCs (Singh et al., 2004).

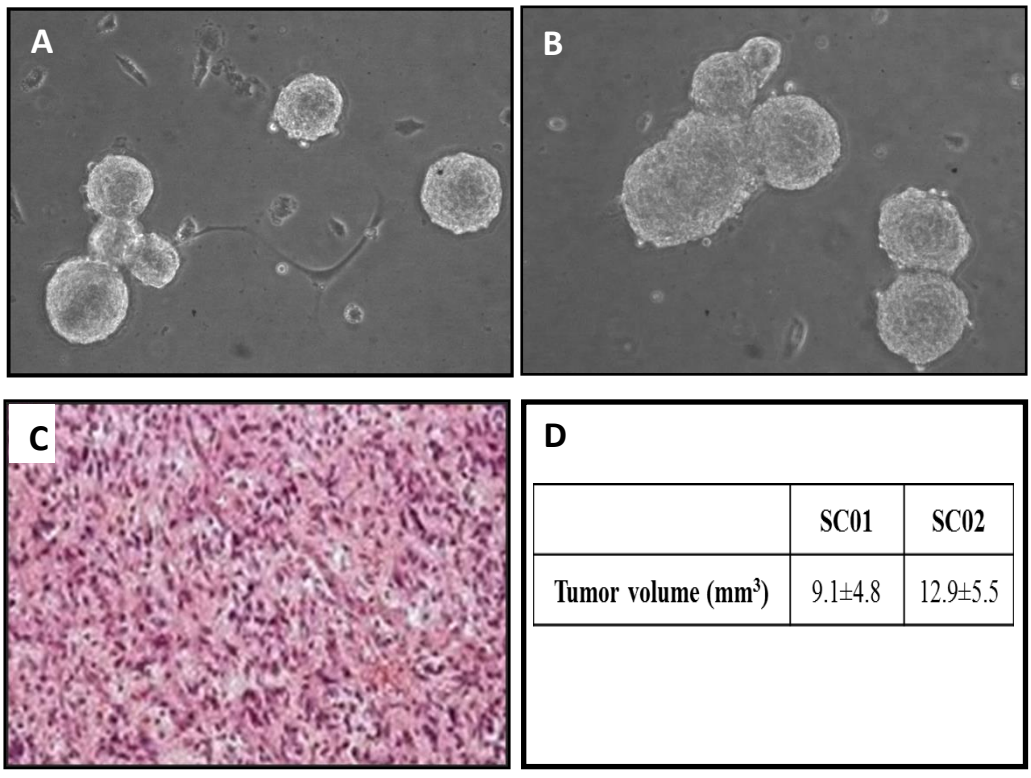

	SC01	SC02
Tumor volume (mm^3)	9.1±4.8	12.9±5.5

FIGURE 6: **Stem cell features of GSC lines.** Representative microscopic image of GSCs grown as neurospheres of (A) slow- and (B) fast-proliferating GSC lines (magnification, 200x). (C) Representative histological image (hematoxylin and eosin staining) and (D) graphic representation of a brain tumor

derived from GSCs after intracranial orthotopic xenograft of nude mice.

5.7 SC01 and SC02 neurospheres differ in the expression of stemness markers

In order to phenotype SC01 and SC02, we determined the expression of different putative stem/progenitor cell markers. As shown in Fig. 7, all the investigated makers were highly expressed in both GSCs, with CD90 as the highest (>90%) expressed one. It should be noted that CD90 has been recently identified as a novel marker for GSCs in high-grade gliomas and as a more general marker than the recognized GSC marker CD133 (He et al., 2012). The expression of all other markers, including CD133 and CD15, was significantly higher in SC02 than SC01.

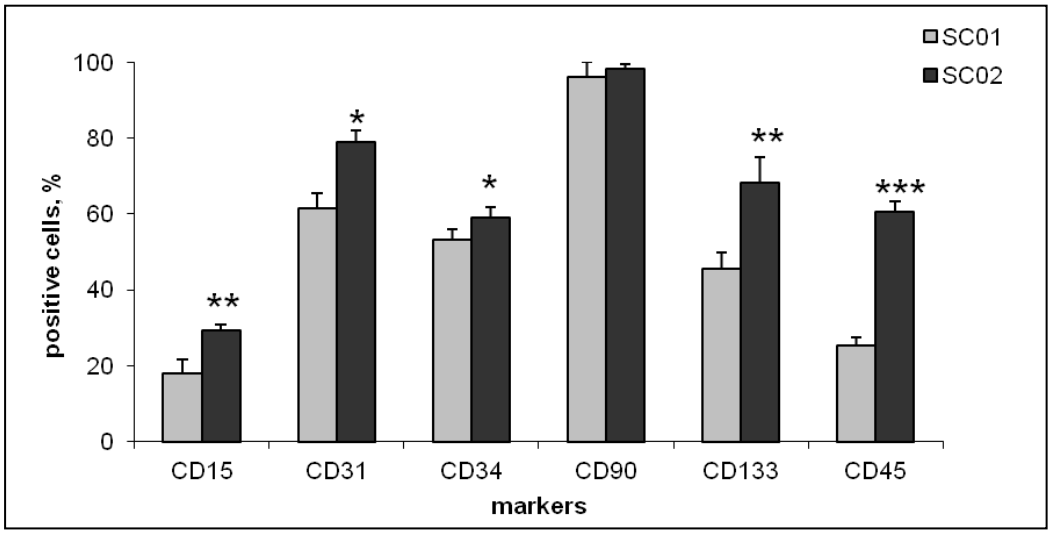

FIGURE 7: Slow- and fast-proliferating GSCs growing as neurospheres differ in stemness marker expression. The expression of different stemness and precursor markers in SC01 (grey) and SC02 (black) cells, obtained by cytofluorimetric analyses is shown. Data are expressed as % of total cells and are the mean ±SD of 3–5 independent experiments. *P<0.05; **P<0.01; ***P<0.001 SC02 versus SC01. Similar data were obtained at different cell passages.

5.8 SC01 and SC02 differ in the proliferation rate and cell cycle parameters

In the used culture condition, the analyses of the cellular growth curves showed that, along with passages, the cell number gradually increased, and this increase was much more pronounced in the SC02 line (Fig. 8A). Moreover, at both 2 and 7 days in culture, the proliferation index was significantly higher in SC02 than SC01 (Fig. 8B).

The results of the cell cycle evaluation by flow cytometry revealed differences in the number of cells undergoing mitosis between the two cell lines. In fact, when compared with SC01 (Fig. 8C), the SC02 cell line (Fig. 8D) exhibited a significant increase in the percentage of cells in the mitotic phases and a decrease in that of cells in G0/G1 phase.

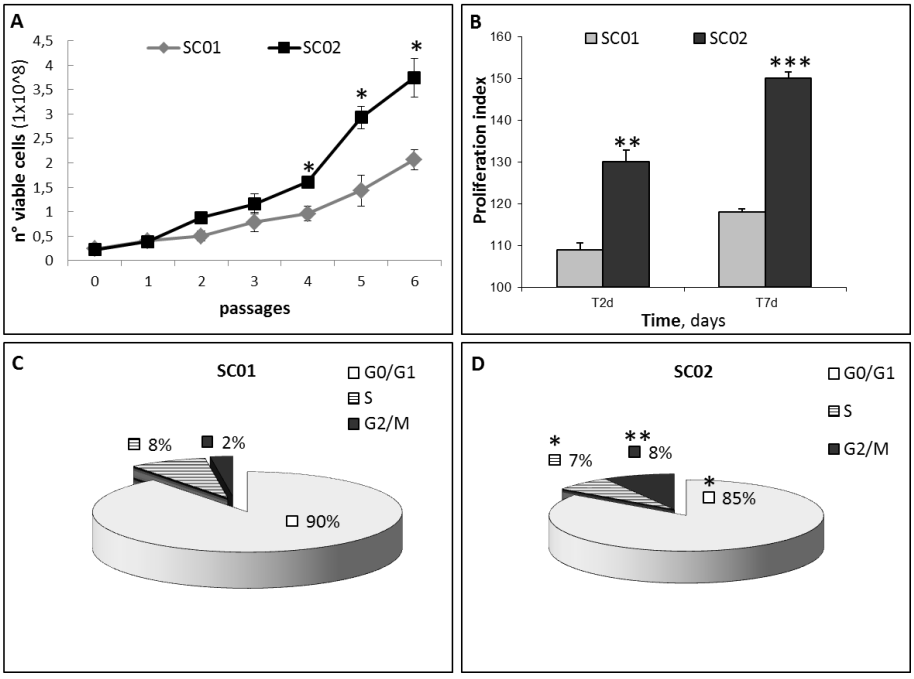

FIGURE 8: Slow- and fast-proliferating GSCs differ in proliferation and cell cycle parameters. (A): SC01 and SC02 were plated at the same initial density, and at each passage viable cells were counted; (B) GSCs at the 5th passage were plated, and after 2 and 7 days in culture, the proliferation index was calculated as described in "Materials and Methods"; GSCs from (C) SC01, and (D) SC02, were plated as above, and cell cycle distribution was analyzed by flow cytometry. Similar data were obtained at different cell passages. *P<0.05; **P<0.01; ***P<0.001, SC02 versus SC01.

5.9 SC01 and SC02 Differ in Sph Metabolism and Extracellular Release of S1P

To follow S1P metabolism and its breakdown product, we used Sph labeled with tritium at the C3 position of the long chain base backbone. This label remains in the lipid throughout the phosphorylation and recycling steps of the sphingoid base, and thus allows tracking of all metabolites as long as the sphingoid backbone remains intact, as well as S1P irreversible degradation as tritiated water. After administration, tritiated Sph was rapidly incorporated into the two GSC lines in a time-dependent fashion, and, after 120 min, total incorporated radioactivity accounted for 197.9±20.7 in SC01, and 214.2±19.8 nCi/dish in SC02, that is approximately half of the administered radioactivity. At all investigated times, the level of intracellular 3H-Sph was found low, representing less than 10% of the total incorporated radioactivity in both cell lines, this level being 3-, 4-fold higher in SC01 than that of SC02 cells (Fig. 9). These data indicate that both GSC types are able to rapidly incorporate and metabolize exogenous Sph, and that the SC02 cells are particularly efficient in this metabolization.

At different pulse times, the bulk of incorporated radioactivity was associated to the N-acylated derivatives of Sph, and, in less amounts, to the 1-phosphorylation products (Fig. 9).

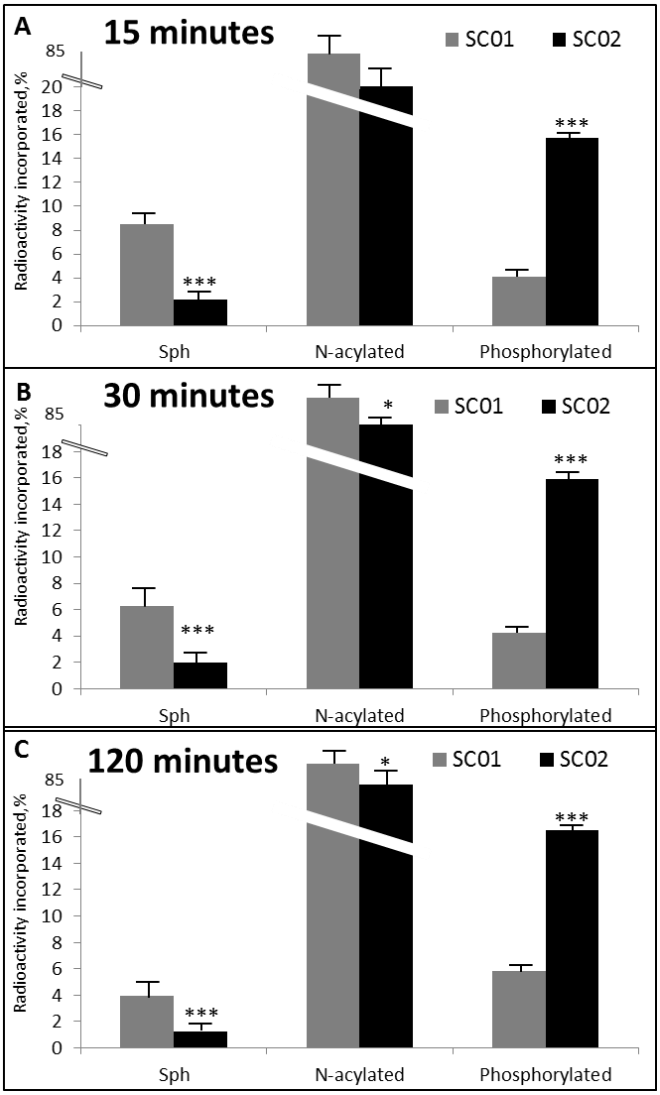

FIGURE 9: Slow- and fast-proliferating GSCs differ in Sph metabolism. SC01 (grey bar) and SC02 (black bar) cells were pulsed with 20 nM 3H-Sph for 15–120 min. At the end, cells and media were processed and analyzed as described in "Materials and Methods". The radioactivity distribution (as % of total incorporated radioactivity) among unmetabolized Sph, and its N-acylation, and 1-phosphorylation products is shown at (A) 15 minutes, (B) 30 minutes, (C) 120 minutes. Data are the mean of three experiments, performed in duplicate. *P < 0.05; ***P < 0.001, SC02 versus SC01.

It is worth noting that the ratio between N-acylated and 1-phosphorylated metabolites was 21.3 and 15.5 in SC01, and 5.2 and 4.9 in SC02 at 15 and 120 min, respectively.

The main N-acylated metabolites produced during pulse in both GSC lines were

represented by Cer and complex sphingolipids, including sphingomyelin, and, in much lower amounts, Glc-Cer. All over pulse, Cer was by far the major ^{3}H-metabolite, its anabolic derivatives increasing with time (Fig. 10). A significant decrease in ^{3}H-Cer in SC02 compared with SC01 was observed after 120 min pulse (Fig. 10A). All over pulse, in SC02 cells a marked elevation of sphingomyelin and Glc-Cer was also evident (Fig. 10B).; at 120 min, in SC02 these sphingolipids increased by about 110% and 250%, respectively, relative to SC01 (Fig. 10C). As reported above, the metabolites derived from the 1-phosphorylation process represented the second class of Sph derivatives (Fig. 9).

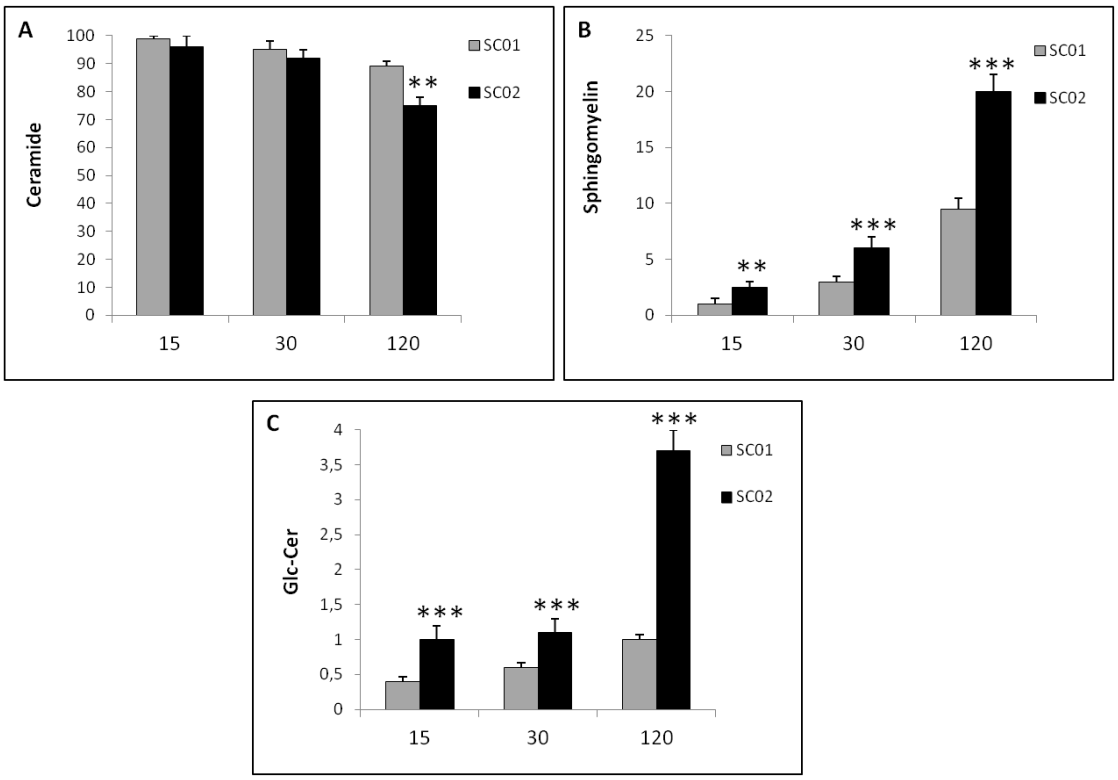

FIGURE 10: Cer consumption to SM and Glc-Cer is enhanced in fast-proliferating GSCs. Content of labeled Cer (A), sphingomyelin (B), and Glc-Cer (C) in SC01 (light grey) and SC02 (dark) at 15–120 min pulse with 3H-Sph. Data are expressed as percent of N-acylated metabolites, and are the mean6SD of 3 experiments. **P < 0.01; ***P < 0.001, SC02 versus SC01.

Among them, intracellular S1P represented only a minor fraction of 1-phosphorylated Sph metabolites and, at 15 min pulse, its level was significantly lower in SC01 than SC02 (Fig. 11A). Thereafter, there was no relevant change in the cellular S1P level between SC01 and SC02. At all investigated times, tritiated water, represented the vast majority of Sph 1-phosphorylation products, its content being significantly higher (4-, 6-fold) in SC02 than in SC01 (Fig. 11B). After pulse with [C3-^{3}H]Sph, tritiated water derives from the oxidation of tritiated hexadecenal produced from ^{3}H-S1P by S1P lyase (Anelli et al., 2005). Our results indicate that a rapid and efficient degradation of S1P, derived from the phosphorylation of exogenous Sph, occurs in GSCs. Besides tritiated water, the analyses of the culture media from both cell lines revealed the presence of labeled S1P (Fig. 11C,D), which increased in a time-dependent fashion in both cell lines. Remarkably, at all investigated times, the S1P levels in the extracellular milieu of SC02 were significantly higher than those of SC01 (Fig. 11C). At 120 min pulse extracellular S1P from SC02 accounted for about 4-fold that of intracellular S1P, and about 9-fold that of SC01 ($P<0.001$).

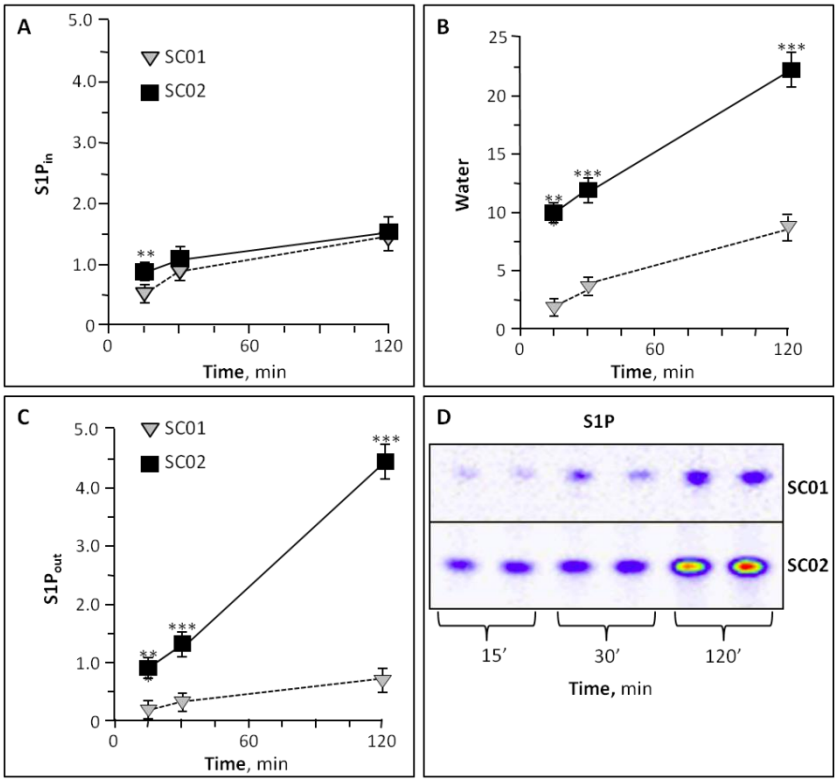

FIGURE 11: Slow- and fast-proliferating GSCs differ in S1P degradation and export. The radioactivity associated to (A) intracellular S1P (S1Pin), (B) water, and (C) extracellular S1P (S1Pout) in SC01 (dotted line) and SC02 (straight line) is shown at 15–120 min pulse with 3H-Sph. Results are expressed as nCi/well, and are the mean6SD of three experiments in duplicate. **P< 0.01; ***P< 0.001, SC02 versus SC01. D: Representative autoradiographic image of the extracellular S1P containing fractions from SC01 and SC02, after 15–120 min pulse.

5.10 Extracellular Secretion of S1P by SC Cells is Highly Efficient and Stimulated by Growth Factors

To better define the S1P export from GSCs, we next addressed the possibility that elevated levels of Sph might influence its metabolism and S1P export. After pulse of GSCs with 1 mM Sph, the percentage of phosphorylated metabolites, including both intracellular S1P and its catabolic product water, increased in respect with the N-acylated ones in both cell lines. In the presence of 1 mM Sph, the amount of released S1P was relevant, reaching on average the concentration

of 2 nM in both cell lines. Since EGF and bFGF are recognized as autocrine signals in GSCs, we then evaluated the possible influence of these growth factors on S1P release. The results demonstrated that either in the absence or presence of EGF and bFGF, GSCs can release S1P, reflecting a constitutive S1P secretion by the cells. It is relevant to note that this secretion was significantly enhanced by the presence of EGF and bFGF (Fig. 12A,B), supporting an autocrine loop induced by these growth factors.

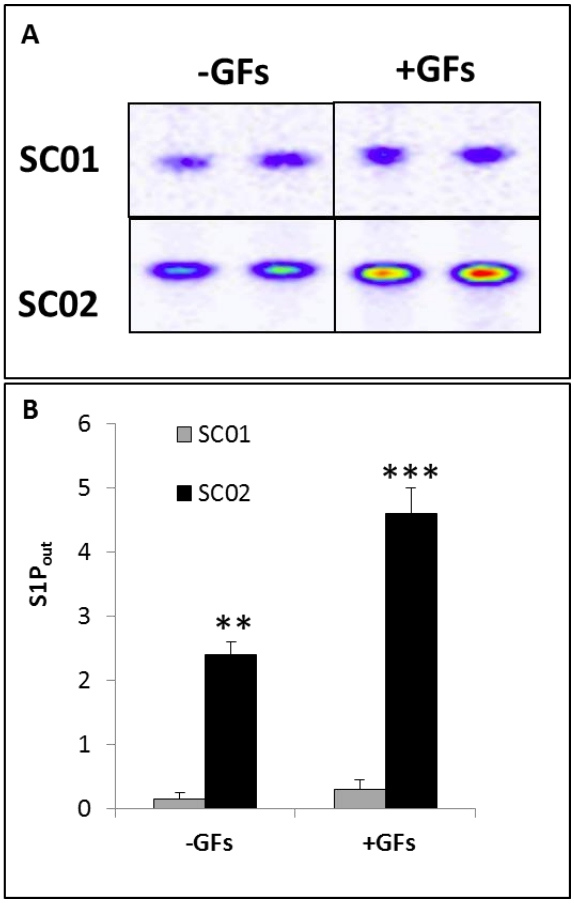

FIGURE 12: Growth factors stimulate S1P export by GSCs. GSCs were pulsed with 20 nM 3H-Sph in SCM without (- GFs) or with (+ GFs) EGF and bFGF for 120 min. A: Representative autoradiographic image of the extracellular S1P containing fractions from SC01 and SC02, separated by HPTLC. B: Radioactivity associated to extracellular S1P (S1Pout) is expressed as nCi/well and is the mean6SD of three experiments. **P<0.01; ***P<0.001,+GFs versus - GFs.

5.11 Extracellular S1P Prompts GSC Proliferation and Stemness

On the basis of the above results, it was of interest to investigate whether extracellular S1P can influence the GSC proliferation index and/or stemness. In this scenario, GSCs were cultured in S1P-enriched SCM medium for 48 h, and the number of viable cells was determined. As shown in Fig. 13A, the addition of S1P resulted in a significant increase in viable cells compared with the control group ($P<0.01$). These results suggest that extracellular S1P promotes GSC survival and/or proliferation. Trypan blue exclusion test revealed that few cells (less than 5%) were stained in control and S1P treated cells. Cytofluorimetric studies were performed. These studies, besides confirming the low level of dead cells in both control and S1P-treated cells, demonstrated that the number of cells in the early and late apoptosis, as well as the necrotic one was significantly reduced after S1P administration (Fig. 13B). However, due to the low levels of death cells, it is unlikely that the increase in cell number in S1P treated cells results from reduced apoptosis/necrosis, and it may indicate an effect on cell cycle progression. We then performed FACS analyses to determine the cell cycle profile in S1P-treated cells. After culturing in S1P-containing medium, quantitative analysis showed that cells in the G0/G1 phase decreased and those in the S and G2/M phases significantly increased (Fig. 13C), suggesting that GSCs cultured in S1P containing medium transitioned from the G1 phase to the S and G2/M phases of the cell cycle. In agreement, we found that the proliferation index of S1P-treated cells was increased significantly in comparison with cells that did not receive the sphingoid molecule, and this effect was inhibited by FTY720 (Fig. 13D). Taken together, these results point out that

extracellular S1P, after binding to S1PRs, promotes GSC survival and proliferation.

In order to evaluate if the proliferating effect of S1P was selective for GSCs or shared with non-stem GBM cells, we prepared primary cultures of GBM cells from tumor samples from pt 1 and 2, and evaluated the effect of S1P on their proliferation. These experiments demonstrated that 200 nM S1P significantly increased the proliferation of GBM cells from pt 1 and pt 2, by 26.8% and 38.2%, respectively (P<0.01 in both cases).

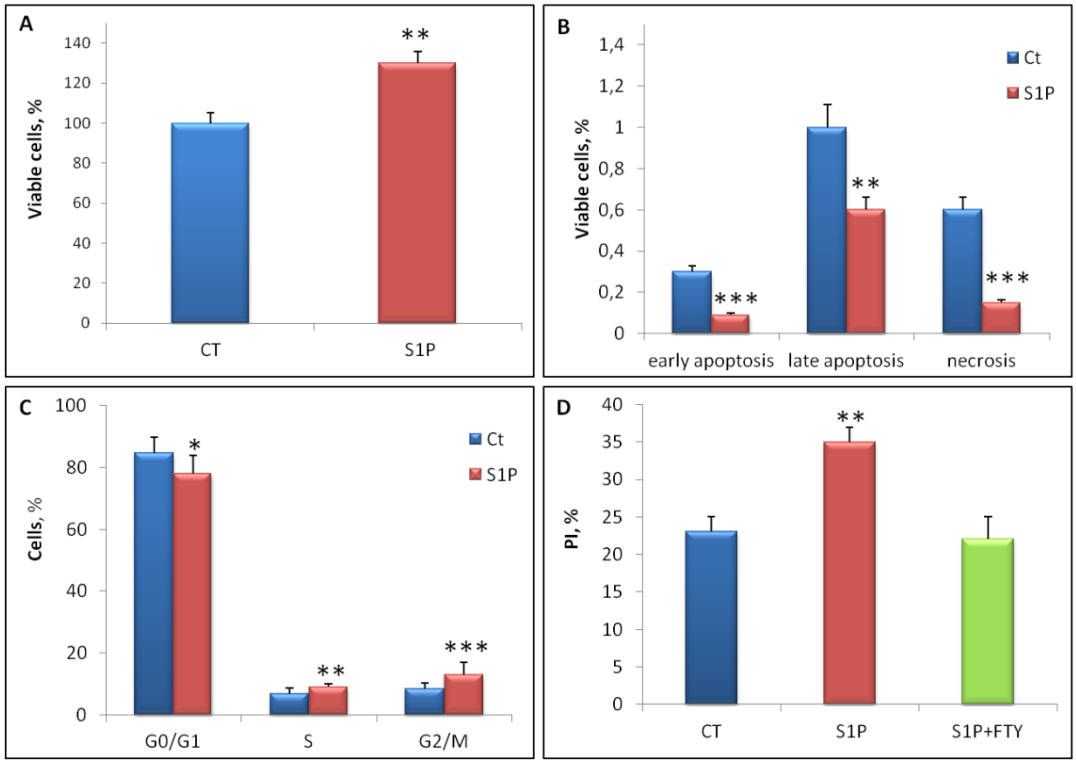

FIGURE 13: Extracellular S1P promotes GSC survival and proliferation. SC02 cells were treated in the absence (Ct) or presence of 200 nM S1P alone (S1P) or with 100 nM FTY720 (S1P1+FTY) for 48 hours. At the end, cell viability (A), apoptosis (B), cell cycle parameters (C), and proliferation index (PI) (D) were assessed as reported in "Materials and Methods". *P<0.05; **P<0.01; ***P<0.001, S1P-treated versus Ct. Similar effects of S1P were obtained on SC01 cells.

Finally, we evaluated the effect of nanomolar concentrations of S1P on cell stemness. Remarkably, the results of the phenotypic characterization by FACS analyses demonstrated that S1P significantly increased the expression of different stemness and precursor markers in GSCs (Fig. 14A), including, among others, CD133 and CD15. This S1P effect could be due to either an induction of stem cell marker expression or a selective expansion of cells that are already expressing stem cell markers. In order to clarify this point, we evaluated the effect of S1P on stem marker expression in primary cultures of GBM cells prepared from pt 1 and 2. We first found that primary GBM cells express very low levels of stemness markers. Indeed, as shown in Fig. 14B, the percentages of CD133 and CD151 cells in GBM cells from pt 2 were by far lower (15- and 25-fold) the corresponding value of SC02, their corresponding GSCs (Fig. 13A). We found similar differences in the stem marker expression by GBM cells from pt 1 and SC01. Of relevance, and differently from what we observed in GSCs, S1P exerted only modest, if any, effect on the stemness profile of primary GBM cells (Fig. 14B).

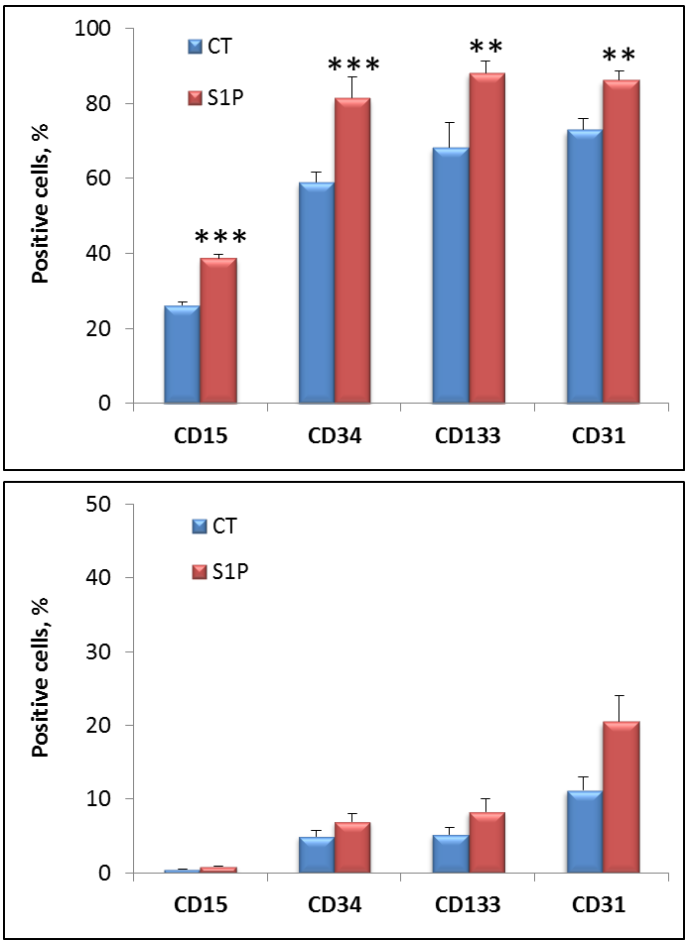

FIGURE 14: Extracellular S1P enhances GSC stemness in GSCs but not in GBM cells. (A) SC02 cells and GBM cells from pt 2 (B) were incubated in the absence (Ct) or presence of 200 nM S1P (S1P) for 48 h. At the end, the immunophenotypic profile was assessed by cytofluorimetric analyses. Results are expressed as percent of total cells and are the mean ± SD of three independent experiments. **P < 0.01; ***P < 0.001, S1P treated versus Ct. Similar effects of S1P were observed on SC01 and GBM cells from pt 1.

5.12 Combined treatment: TMZ and FTY720 induced GSC death through the activation of autophagic death.

We next speculated that FTY720 might augment the effect of TMZ on GSC lines, and that GCS might be involved in TMZ resistance. To test this hypothesis, we first analysed the effect of TMZ alone on SC01 and SC02 cell lines. Cells were plated on permanox glass chamber slide in SCM medium

(Figure 15A) and were treated with 100µM of TMZ alone (Figure 15B) or in combination with 3µM of FTY720 (Figure 15C). Images obtained by phase contrast microscopy after 48 hours treatment with showed that SC01 and SC02 cell lines maintained unchanged their morphological features. We found that the exposure of resistant cells to a 100µM dose of TMZ, did not affect cell viability after 48h (Figure 15D).

In order to confirm that the real effects was related to S1P production and release, we explored the effect of combination treatment (TMZ plus FTY720) on drug sensitivity. The results showed that the incubation with either TMZ and FTY720 lead to a significant reduction in cell viability both SC01 and SC02 GSC lines.

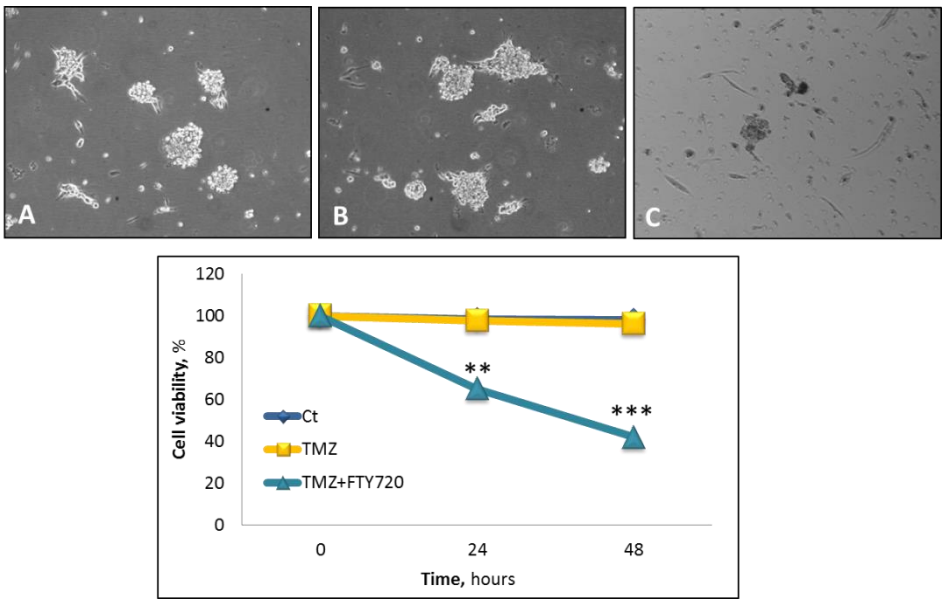

FIGURE 15: Effect of TMZ on cell survival. Representative images of GSCs morphology after 48 h treatment with vehicle (A, 0.1% DMSO) or 100 µM TMZ (B) alone, or in combination with 3µM FTY720 (C). Images were viewed on a phase contrast microscope, and digital images were acquired (magnification, 100X). (D) GSCs were exposed to TMZ and FTY720 or vehicle. Cell viability was assessed after 48 h of treatment by MTT assay. Results are expressed as percentage of cell viability with respect to vehicle-treated cells (100%). Data are the mean ± SD of three independent experiments. * $p < 0.05$; ** $p < 0.01$ vs vehicle-treated cells.

Recent studies demonstrated that TMZ-induced autophagy in apoptosis-resistant GBM cells (Zhang J, et al., 2015) can be the result of the activation of authophagic process. To evaluate whether the combination with TMZ and FTY720 of the exposed cells induce autophagy, we performed cell staining with acridine orange, in parallel to Hoechst 33342 after drug treatments.

Results revealed that after 48 hours, no formation of acidic vesicular organelles was evident in GSC lines without treatment (Figure 16A-D), whrease, in TMZ-treated cells, acridine orange staining showed an increase in the number, size, and strength of the bright red fluorescence spots in the cytoplasm (Figure 16E-H) and this increase trend was observed with significant evidence in TMZ+FTY720 combined GSC-treated (Figure 16I-L).

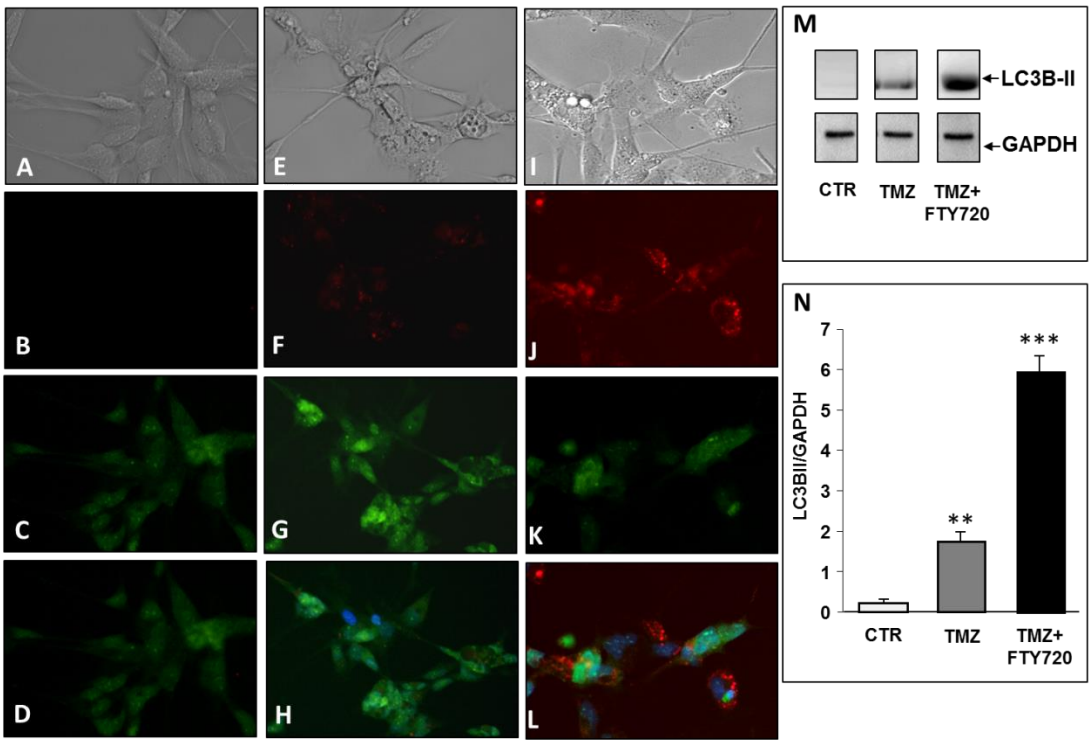

FIGURE 16: FTY720 in combination with TMZ induces autophagic death in GSCs cells. Vital staining with Hoechst 33342 and acridine orange of GSCs treated with vehicle, (A-D), with 100μM TMZ alone (E-H), or in combination with 3μM FTY720 (I-L) for 48 hours. The fluorescence microscopy images

(original magnification, 400x) are representative of control and treated cells observed in three independent experiments. (M) Cell lysates (60 μg of proteins) were analysed by immunoblotting with anti-LC3B and anti-GAPDH antibodies. Similar expression was obtained in several independent experiments. (N) Quantification of LC3B-II expression versus GAPDH expression in GSCs treated with vehicle, TMZ alone or in combination with FTY720. Data are the mean ± SD of three independent experiments. $**P<0.01$; $***P<0.001$.

To validate this finding, the expression level of the isoform II of the microtubule associated protein 1 light-chain 3B (LC3B-II), a recognized marker of autophagy (31), was assessed. As shown in Figure 14M, the treatment with TMZ induced a significant increase in the LC3B-II protein. Furthermore, the incubation with TMZ and FTY720, showed a more significant increased trend, this level being 6-fold higher in combination treatment than that the vehicle one, thus confirming that TMZ+FTY720 induces autophagic death in GSC lines.

DISCUSSION

Glioblastoma multiforme is the most common primary malignant brain tumor in adults and with the worst prognosis (Louis DN, et al., 2007). Several clinical predictors of survival have been identified, such as age, pre-operative functional status and tumor extent (Gorlia T, et al., 2008). In addition, some genetic and epigenetic features may be used as prognostic factors (van den Bent MJ, et al., 2010; van den Bent MJ, et al., 2009). Nevertheless, despite many efforts to treat this disease, the mortality rate remains high, recurrence seems to be the rule and still the outcome is invariably fatal. In this light, a better understanding of the biological background of tumor growth and aggressiveness in patients with gliomas may be helpful to identify targeted therapies to achieve a better outcome. Malignant transformation results from the sequential accumulation of genetic alterations and abnormal regulation of growth factors signalling mediated also by sphingolipids. Moreover, the finding of a subpopulation of CSCs is present in the core of the tumor, has fuelled the hypothesis that these cells play a crucial role in proliferation, aggressiveness, and intrinsic resistance to therapy, being thus a key determinant driving tumor growth and relapse after resection (Baronchelli S, et al., 2013; Marfia G, et al., 2014). The standard of care for patients with newly diagnosed GBM includes maximal safe resection of the tumor followed by 6 week course of Radio therapy (RT) with concomitant systemic therapy using alkylating agent TMZ (Stupp et al., 2005 Stupp et al., 2008; Weller M, et al., 2014). This combination has increased the survival of patients with GBM, but their median survival remains only about 15 months (Ohgaki H & Kleihues P. 2005). Standard of care approach is generally uniform and does not take into account different molecular and biological signatures of

GBM. Our study provides a contribution to this complex field.

Indeed, a central unresolved issue with GSCs is their growth signaling and cell cycle control that are different from patient to patient. This lack of progress is especially surprising given that the histopathological assessment in the diagnosis of GBM includes the identification of a high tumor cell mitotic index (Persano et al., 2013; Pojo & Costa, 2011), as well as that a key determinant of GSCs is their capacity for extensive proliferation and self-renewing (Al-Hajj et al., 2004; Oliver and Wechsler-Reya, 2004).

S1P is increasingly recognized as a critical growth factor for a number of cancer cell types and, among others, glioma cells (Yester et al., 2011). A role for S1P as a potential mitogenic factor in GSCs, however, remains uncharacterized. In this research project overall 57 patients who underwent neurosurgical procedures for GBM between February 2012 and June 2015 were included in the study. All patients underwent surgical resection of the lesion. Interesting, the tumor volume was significantly bigger in patients who died than in those who were survivors at the end of the follow-up period (median 32.5 vs 23.4 cm3; IQR: 16.3-53.0 vs 6.4-35.0, respectively; p=0.04).

To this purpose we investigated the origin and role for S1P in GSC properties and specifically in GSC proliferation and stemness. Among different 30 GSC lines prepared from 57 GBM specimens, on the bases of proliferation and stemness parameters, we selected two cell lines, named SC01 and SC02, as representative of slow- and fast-proliferating cells, respectively. Moreover the finding that both GSCs, in addition to the well-known stemness markers, express CD31, CD34, CD45, is in agreement with previous evidence in literature, suggesting that CD133+ cells could have an intrinsic differentiation potential

toward tumor cells or endothelial cells (Christensen et al., 2011; He et al., 2012). These GSC populations demonstrated heterogeneity not only in terms of proliferative potential, but also of expression of stem cell markers, the fast proliferative status of SC02 being paralleled by a higher expression of stemness and angiogenic parameters.

It is becoming increasingly clear that GSC properties involve a complex interplay between GSCs and their microenvironment, and the GSC microenvironment provides essential cues to their maintenance (Charles et al., 2012; Filatova et al., 2013; Heddleston et al., 2011). Further results here obtained underscore the relevance of the extracellular environment in affecting the extent of S1P export.

Indeed, metabolic studies revealed that both GSC lines were able to efficiently take up and metabolize Sph, but with significant differences between slow-proliferating and fast-proliferating cells. In particular, SC02 exhibited an extremely rapid Sph processing, and a significant higher ratio between 1-phosphorylated and N-acylated metabolites than SC01, indicating that in the two cell lines a different propensity exists in the use of Sph by the two different metabolic routes. Moreover, we show that the two cell types had different kinetics of Cer consumption. Both types of Cer consumption, which convert Cer to SM and GlcCer were potentiated in SC02, and appear functional to avoid Cer accumulation in these cells. A further result of the metabolic experiments was that GSCs constitutively exhibit the property to efficiently release S1P in the extracellular microenvironment, in line with previous recent study (Riccitelli E, et al., 2013). The novel finding is that the proliferative properties of GSCs appeared as related to efficient and rapid release of newly produced S1P. Indeed

extracellular S1P level was up to 10-fold higher in SC02 than SC01, suggesting that the high extent of S1P release by SC02 cells reflects, and most probably participates, in their proliferation and stemness features. In spite representative of different GSC lines, the limited number of GSC lines here used and the heterogeneity of GMBs warrant further studies to confirm these findings.

Overall, these metabolic experiments demonstrate that fast proliferating cells exhibit an increased flux through the pathway converting Sph to S1P, paralleled by an increase of Cer to complex sphingolipids, the most relevant changes being gain of extracellular S1P and loss of intracellular Sph and Cer. Since the balance between S1P and Cer/Sph levels is believed to provide a rheostat mechanism determinant for cell proliferation and fate (Spiegel & Merrill, 1996), our results suggest that altering this rheostat in favor of S1P provides SC02 an advantage in their proliferative and stemness qualities. In agreement, a decrease in total ceramides and an increase in S1P content with increasing glioma grade were reported (Abuhusain et al., 2013; Riboni et al., 2002).

Further results here obtained underscore the relevance of the extracellular environment in affecting the extent of S1P export. The finding that S1P promotes stemness parameters in GSCs, might reside in its ability to promote either the expression of different stem markers or the proliferation of GSCs that are already expressing stem cell markers. In non-stem primary GBM cells, we observed that S1P did not induce stemness marker expression, thus suggesting that its effect resides in the selective expansion of GSCs.

We observed that S1P treatment resulted in elevation of the CD133+ population of GSCs. It is worth noting that this subpopulation of GSCs was demonstrated to present a more malignant behaviour, and is able to maintain the GSC pool in the

tumor, also increasing its cellular heterogeneity (Lathia et al., 2011b; Zeppernick et al., 2008). Although at present the mechanisms of the stemness-promoting action of S1P are unknown, it appears reasonable that the S1P might induce the expansion of CD133+ GSCs, and/or their dedifferentiation to CD133+ GSCs. Of interest, besides CD133+ cells, S1P increased the CD15+ population too, and this population was reported to complement some part of CD133 function, as it survives better and proliferates faster than their negative counterpart (Zeppernick et al., 2008). We found that S1P also increased the number of cells expressing the hematopoietic/endothelial progenitor markers CD31+and CD34+. Intriguingly, CD31+ and CD34+ GSCs were found to co-express CD133+, and to be more proliferating than the negative counterpart (Christensen et al., 2011). Overall, these data suggest that fast-proliferating GSCs possess a high propensity for secreting S1P, and that autocrine S1P acts as microenvironmental signal to increase the GSC population and to enhance their stem cell properties. Besides emphasizing the importance of S1P as a proliferative factor, this study underscores S1P export as a crucial step in connecting GSCs with their niche, and suggests that S1P secretion by GSCs may also have the effect of targeting functions of nonstem niche cells in a paracrine manner. In line with this, S1P has been reported to favour propagation of non-stem cell types present in the GSC niche, such as astrocytes (Bassi et al., 2006), endothelial cells (Rosen et al., 2005), and as confirmed in our study, in non-stem glioma cells, too (Van Brocklyn et al., 2002; Yoshida et al., 2010). Additionally, our results revealed that FTY720, when administrated in combination with the chemotherapeutic agent TMZ, sensibilized GSCs to chemotherapy enhancing autophagic death. As previously described by Estrada-Bernal and collaborators, FTY720 treatment of

brain tumor stem cells from GBM led to rapid inactivation of ERK MAP kinase, leading to apoptosis in combination with TMZ. In *in vivo* mouse model of GBM, FTY720 augmented the therapeutic effect of TMZ, increasing the survival rate (Estrada-Bernal A, et al., 2012). FTY720 received Food and Drug Administration approval for treatment of relapsing multiple sclerosis and, thus, has been shown to be well-tolerated in human patients and to enter the central nervous system. All in all, this research project showed significantly results regarding the involvement of sphingolipids in conferring resistance to GSCs. Hence, not only genetic and epigenetic modifications can play a key role in the progression, aggressiveness and recurrence of the disease, but also metabolic changes may adversely affect the development of this malignant tumor.

These findings have provided a compelling rationale for involvement of S1P receptor antagonists, as a new approach to anticancer drug development.

REFERENCES

Abuhusain HJ, Matin A, Qiao Q, Shen H, Kain N, Day BW, Stringer BW, Daniels B, Laaksonen MA, Teo C, McDonald KL, Don AS. A metabolic shift favoring sphingosine 1-phosphate at the expense of ceramide controls glioblastoma angiogenesis. J Biol Chem. 2013;288:37355–37364.

Adamson DC, Rasheed BA, McLendon RE, Bigner DD. Central nervous system. Cancer Biomark. 2010;9:193-210.

Adan-Gokbulut A, Kartal-Yandim M, Iskender G, Baran Y. Novel agents targeting bioactive sphingolipids for the treatment of cancer. Curr Med Chem. 2013;20:108–122.

Ader I, Brizuela L, Bouquerel P, Malavaud B, Cuvillier O. Sphingosine kinase 1: a new modulator of hypoxia inducible factor 1α during hypoxia in human cancer cells. Cancer Res. 2008;68:8635–8642.

Al-Hajj M, Becker MW, Wicha M, Weissman I, Clarke MF. Therapeutic implications of cancer stem cells. Curr Opin Genet Dev. 2004;14:43–47.

Anelli V, Bassi R, Tettamanti G, Viani P, Riboni L. Extracellular release of newly synthesized sphingosine-1-phosphate by cerebellar granule cells and astrocytes. J Neurochem. 2005;92:1204–1215.

Anelli V, Gault CR, Cheng AB, Obeid LM. Sphingosine kinase 1 is up-regulated during hypoxia in U87MG glioma cells. Role of hypoxia-inducible factors 1 and 2. J Biol Chem. 2008;283:3365–3337.

Anelli V, Gault CR, Snider AJ, Obeid LM. Role of sphingosine kinase-1 in paracrine/transcellular angiogenesis and lymphangiogenesis in vitro. FASEB J. 2010;24:2727–2738.

Asthagiri AR, Pouratian N, Sherman J, Ahmed G, Shaffrey ME. Advances in brain tumor surgery. Neurol Clin. 2007;25:975-1003.

Bao S, Wu Q, McLendon RE, Hao Y, Shi Q, Hjelmeland AB, Dewhirst MW, Bigner DD, Rich JN. Glioma stem cells promote radioresistance by preferential activation of the DNA damage response. Nature. 2006;7;444:756-60.

Barceló-Coblijn G, Martin ML, de Almeida RF, Noguera-Salvà MA, Marcilla-Etxenike A, Guardiola-Serrano F, Lüth A, Kleuser B, Halver JE, Escribá PV. Sphingomyelin and sphingomyelin synthase (SMS) in the malignant transformation of glioma cells and in 2-hydroxyoleic acid therapy. Proc Natl Acad Sci U S A. 2011;108:19569–19574.

Barker FG 2nd, Prados MD, Chang SM, Gutin PH, Lamborn KR, Larson DA, Malec MK, McDermott MW, Sneed PK, Wara WM, Wilson CB. Radiation response and survival time in patients with glioblastoma multiforme. J Neurosurg. 1996;84:442-448.

Baronchelli S, Bentivegna A, Redaelli S, Riva G, Butta V, Paoletta L, Isimbaldi G, Miozzo M, Tabano S, Daga A, Marubbi D, Cattaneo M, Biunno I, Dalprà L. Delineating the cytogenomic and epigenomic landscapes of glioma stem cell lines. PLoS One. 2013;8:e57462.

Beauchesne P. Fotemustine: a third-generation nitrosourea for the treatment of recurrent malignant gliomas. Cancers (Basel). 2012;4:77-87.

Beier D, Hau P, Proescholdt M, Lohmeier A, Wischhusen J, Oefner PJ, Aigner L, Brawanski A, Bogdahn U, Beier CP. CD133(+) and CD133(-) glioblastoma-derived cancer stem cells show differential growth characteristics and molecular profiles. Cancer Res. 2007:4010-5.

Bolduc JM, Dyer DH, Scott WG, Singer P, Sweet RM, Koshland DE Jr, Stoddard BL. Mutagenesis and Laue structures of enzyme intermediates: isocitrate dehydrogenase. Science. 1995;268:1312-1318.

Buckner JC, Brown PD, O'Neill BP, Meyer FB, Wetmore CJ, Uhm JH. Central nervous system tumors. Mayo Clin Proc. 2007;82:1271-86.

Campanella R. Membrane lipid modifications in human gliomas of different degree of malignancy. J Neurosurg Sci. 1992;36:11–25.

Charles NA, Holland EC, Gilbertson R, Glass R, Kettenmann H. The brain tumor microenvironment. Glia. 2012;60(3):502-14. Review.

Choucair AK, Levin VA, Gutin PH, Davis RL, Silver P, Edwards MS, Wilson CB. Development of multiple lesions during radiation therapy and chemotherapy in patients with gliomas. J Neurosurg. 1986;65:654-658.

Christensen K, Schrder HD, Kristensen BW. CD133+ niches and single cells in glioblastoma have different phenotypes. Neuro Oncol. 2011;104:129–143.

Cuvillier O, Pirianov G, Kleuser B, Vanek PG, Coso OA, Gutkind S, Spiegel S. Suppression of ceramide-mediated programmed cell death by sphingosine-1-phosphate. Nature. 1996;381, 800–803.

Dick JE. Stem cell concepts renew cancer research. Blood. 2008;112:4793–4807.

Dolecek TA, Propp JM, Stroup NE, Kruchko C. CBTRUS statistical report: primary brain and central nervous system tumors diagnosed in the United States in 2005-2009. Neuro Oncol. 2012;14:1-49.

Estrada-Bernal A, Palanichamy K, Ray Chaudhury A, Van Brocklyn JR. Induction of brain tumor stem cell apoptosis by FTY720: a potential therapeutic agent for glioblastoma. Neuro Oncol. 2012;14:405-415.

Filatova A, Acker T, Garvalov BK The cancer stem cell niche(s): the crosstalk between glioma stem cells and their microenvironment. Biochim Biophys Acta. 2013;1830:2496–2508.

Filatova A, Acker T, Garvalov BK. The cancer stem cell niche(s): The crosstalk between glioma stem cells and their microenvironment. Biochim Biophys Acta. 2013;830:2496–2508.

Forsythe JA, Jiang BH, Iyer NV, Agani F, Leung SW, Koos RD, Semenza GL. Activation of vascular endothelial growth factor gene transcription by hypoxia-inducible factor 1. Mol Cell Biol. 1996;16:4604-4613.

Futerman AH, Hannun YA. The complex life of simple sphingolipids. EMBO. 2004;Rep 5: 777-782.

Gaspar LE, Fisher BJ, Macdonald DR, LeBer DV, Halperin EC, Schold SC Jr, Cairncross JG. Supratentorial malignant glioma: patterns of recurrence and implications for external beam local treatment. Int J Radiat Oncol Biol Phys. 1992;24(1):55-7.

Gilbert MR, Wang M, Aldape KD, Stupp R, Hegi ME, Jaeckle KA, Armstrong TS, Wefel JS, Won M, Blumenthal DT, Mahajan A, Schultz CJ, Erridge S, Baumert B, Hopkins KI, Tzuk-Shina T, Brown PD, Chakravarti A, Curran WJ Jr, Mehta MP. Dose-dense temozolomide for newly diagnosed glioblastoma: a randomized phase III clinical trial. J Clin Oncol. 2013;31:4085-4091.

Giussani P, T Colleoni, L Brioschi, R Bassi, K Hanada, G Tettamanti, L Riboni, P Viani. Ceramide traffic in C6 glioma cells: evidence for CERT-dependent and independent transport from ER to the Golgi apparatus.. Biochimica et Biophysica Acta. 2008;1781:40-51.

Gorlia T, van den Bent MJ, Hegi ME, Mirimanoff RO, Weller M, Cairncross JG, Eisenhauer E, Belanger K, Brandes AA, Allgeier A, Lacombe D, Stupp R. Nomograms for predicting survival of patients with newly diagnosed glioblastoma: prognostic factor analysis of EORTC and NCIC trial 26981-22981/CE.3. Lancet Oncol. 2008;9:29-38.

Gupta MK, Qin RY. Mechanism and its regulation of tumor-induced angiogenesis. World J Gastroenterol. 2003;9:1144-55. Review.

Hadjipanayis CG, Van Meir EG. Brain cancer propagating cells: biology, genetics and targeted therapies. Trends Mol Med. 2009;15:519-30. Review.

Hanahan D, Folkman J. Patterns and emerging mechanisms of the angiogenic switch during tumorigenesis. Cell. 1996;86:353-364. Review.

Hannun YA, Obeid LM. Principles of bioactive lipid signalling: lessons from sphingolipids. Nat Rev Mol Cell Biol. 2008;9:139-150.

He J, Liu Y, Zhu T, Zhu J, Dimeco F, Vescovi AL, Heth JA, Muraszko KM, Fan X, Lubman DM. CD90 is identified as a candidate marker for cancer stem cells in primary high-grade gliomas using tissue microarrays. Mol Cell Proteomics. 2012;11:M111.010744.

He J, Liu Y, Zhu T, Zhu J, DiMeco F, Vescovi AL, Heth JA, Muraszko KM, Fan X, Lubman DM. CD90 is identified as a marker for cancer stem cells in primary high grade gliomas using tissue microarrays. Mol Cell Proteomics. 2012;11:1–8.

Heddleston JM, Hitomi M, Venere M, Flavahan WA, Yan K, Kim Y, Minhas S, Rich JN, Hjelmeland AB. Glioma stem cell maintenance: The role of the microenvironment. Curr Pharm Des. 2011;17:2386–2401.

Hegi ME, Diserens AC, Gorlia T, Hamou MF, de Tribolet N, Weller M, Kros JM, Hainfellner JA, Mason W, Mariani L, Bromberg JE, Hau P, Mirimanoff RO, Cairncross JG, Janzer RC, Stupp R. MGMT gene silencing and benefit from temozolomide in glioblastoma. N Engl J Med. 2005;352:997-1003.

Homma T, Fukushima T, Vaccarella S, Yonekawa Y, Di Patre PL, Franceschi S, Ohgaki H. Correlation among pathology, genotype, and patient outcomes in glioblastoma. J Neuropathol Exp Neurol. 2006;65:846-854.

Ichimura K, Schmidt EE, Miyakawa A, Goike HM, Collins VP. Distinct patterns of deletion on 10p and 10q suggest involvement of multiple tumor suppressor genes in the development of astrocytic gliomas of different malignancy grades. Genes Chromosomes Cancer. 1998;22:9-15.

Ignatova TN, Kukekov VG, Laywell ED, Suslov ON, Vrionis FD, Steindler DA. Human cortical glial tumors contain neural stem-like cells expressing astroglial and neuronal markers in vitro. Glia. 2002;39:193-206.

Inoue A, Tanaka J, Takahashi H, Kohno S, Ohue S, Umakoshi A, Gotoh K, Ohnishi T. Blood vessels expressing CD90 in human and rat brain tumors. Neuropathology. 2015 Sep 9.

Jenkins RB, Blair H, Ballman KV, Giannini C, Arusell RM, Law M, Flynn H, Passe S, Felten S, Brown PD, Shaw EG, Buckner JC. A t(1;19)(q10;p10) mediates the combined deletions of 1p and 19q and predicts a better prognosis of patients with oligodendroglioma. Cancer Res. 2006;66:9852-9861.

Jensen SA, Calvert AE, Volpert G, Kouri FM, Hurley LA, Luciano JP, Wu Y, Chalastanis A, Futerman AH, Stegh AH. Bcl2L13 is a ceramide synthase inhibitor in glioblastoma. Proc Natl Acad Sci U S A. 2014 Apr 15;111(15):5682-7. Bcl2L13 is a ceramide synthase inhibitor in glioblastoma. Proc Natl Acad Sci U S A. 2014;111:5682–5687.

Johnson MD, Vnencak-Jones CL, Toms SA, Moots PM, Weil R., Allelic losses in oligodendroglial and oligodendroglioma-like neoplasms: analysis using microsatellite repeats and polymerase chain reaction., Arch Pathol Lab Med. 2003;127:1573-1579.

Jordan CT, Guzman ML, Noble M. Cancer stem cells. N Engl J Med. 2006;355:1253-61. Review.

Jośko J, Gwóźdź B, Jedrzejowska-Szypułka H, Hendryk S. Vascular endothelial growth factor (VEGF) and its effect on angiogenesis. Med Sci Monit. 2000;6:1047-52. Review.

Kappos L, O'Connor P, Radue EW, Polman C, Hohlfeld R, Selmaj K, Ritter S, Schlosshauer R, von Rosenstiel P, Zhang-Auberson L, Francis G. A placebo-controlled trial of oral fingolimod in relapsing multiple sclerosis. N Engl J Med. 2010;362:387–401.

Karahatay S, Thomas K, Koybasi S et al. Clinical relevance of ceramide metabolism in the pathogenesis of human head and neck squamous cell carcinoma (HNSCC): attenuation of C(18)-ceramide in HNSCC tumors correlates with lymphovascular invasion and nodal metastasis. Cancer Lett. 2007;256:101–111.

Kenney-Herbert E, Al-Mayhani T, Piccirillo SG, Fowler J, Spiteri I, Jones P, Watts C. CD15 Expression Does Not Identify a Phenotypically or Genetically Distinct Glioblastoma Population. Stem Cells Transl Med. 2015;4:822-831.

Kimura A, Ohmori T, Ohkawa R, Madoiwa S, Mimuro J, Murakami T, Kobayashi E, Hoshino Y, Yatomi Y, Sakata Y. Essential roles of sphingosine 1-phosphate/S1P1 receptor axis in the migration of neural stem cells toward a site of spinal cord injury. Stem Cells. 2007;25:115–124.

Krex D, Klink B, Hartmann C, von Deimling A, Pietsch T, Simon M, Sabel M, Steinbach JP, Heese O, Reifenberger G, Weller M, Schackert G. Long-term survival with glioblastoma multiforme. Brain. 2007;130:2596–2606.

Lathia JD, Hitomi M, Gallagher J, Gadani SP, Adkins J, Vasanji A, Liu L, Eyler CE, Heddleston JM, Wu Q, Minhas S, Soeda A, Hoeppner DJ, Ravin R, McKay RD, McLendon RE, Corbeil D, Chenn A, Hjelmeland AB, Park DM, Rich JN. Distribution of CD133 reveals glioma stem cells self-renew through symmetric and asymmetric cell divisions. Cell Death Dis. 2011;1:2:e200.

Le Stunff H, Giussani P, Maceyka M, Lépine S, Milstien S, Spiegel S. Recycling of sphingosine is regulated by the concerted actions of sphingosine-1-phosphate phosphohydrolase 1 and sphingosine kinase 2. J Biol Chem. 2007;282:34372–34380.

Le Stunff H, Milstien S, Spiegel S. Generation and metabolism of bioactive sphingosine-1-phosphate. J Cell Biochem. 2004;92:882-899.

Li J, Guan HY, Gong LY, Song LB, Zhang N, Wu J, Yuan J, Zheng YJ, Huang ZS, Li M. Clinical significance of sphingosine kinase-1 expression in human astrocytomas progression and overall patient survival. Clin Cancer Res. 2008;14:6996–7000.

Li Z, Wang H, Eyler CE, Hjelmeland AB, Rich JN. Turning cancer stem cells inside out: an exploration of glioma stem cell signaling pathways. J Biol Chem. 2009;19:284:16705-16709.

Liu H, Chakravarty D, Maceyka M, Milstien S, Spiegel S. Sphingosine kinases: a novel family of lipid kinases. Prog Nucleic Acid Res Mol Biol. 2002;71:493-511.

Liu Y, Wada R, Yamashita T, Mi Y, Deng CX, Hobson JP, Rosenfeldt HM, Nava VE, Chae SS, Lee MJ, Liu CH, Hla T, Spiegel S, Proia RL. Edg-1, the G protein-coupled receptor for sphingosine-1-phosphate, is essential for vascular maturation. J Clin Invest. 2000;106:951–961.

Louis DN, Ohgaki H, Wiestler OD, Cavenee WK, Burger PC, Jouvet A, Scheithauer BW, Kleihues P. The 2007 WHO classification of tumours of the central nervous system. Acta Neuropathol. 2007;114:97-109.

Mao JM, Liu J, Guo G, Mao XG, Li CX. Glioblastoma vasculogenic mimicry: signaling pathways progression and potential anti-angiogenesis targets. Biomark Res. 2015;8;3:8

Marfia G, Campanella R, Navone SE, Di Vito C, Riccitelli E, Hadi LA, Bornati A, de Rezende G, Giussani P, Tringali C, Viani P, Rampini P, Alessandri G, Parati E, Riboni L. Autocrine/paracrine sphingosine-1-phosphate fuels proliferative and stemness qualities of glioblastoma stem cells. Glia. 2014;62:1968-1981.

Marfia G, Campanella R, Navone SE, Di Vito C, Riccitelli E, Hadi LA, Bornati A, de Rezende G, Giussani P, Tringali C, Viani P, Rampini P, Alessandri G, Parati E, Riboni L. Autocrine/paracrine sphingosine-1-phosphate fuels proliferative and stemness qualities of glioblastoma stem cells. Glia. 2014;62:1968-1981.

Merrill AH Jr, Stokes TH, Momin A, Park H, Portz BJ, Kelly S, Wang E, Sullards MC, Wang MD. Sphingolipidomics: a valuable tool for understanding the roles of sphingolipids in biology and disease. J Lipid Res. 2009;50:S97–S102.

Mignard V, Lalier L, Paris F, Vallette FM. Bioactive lipids and the control of Bax pro-apoptotic activity. Cell Death Dis. 2014 29;5:e1266.

Mora R, Dokic I, Kees T, Hüber CM, Keitel D, Geibig R, Brügge B, Zentgraf H, Brady NR, Régnier-Vigouroux A. Sphingolipid rheostat alterations related to transformation can be exploited for specific induction of lysosomal cell death in murine and human glioma. Glia. 2010;58:1364–1383

Nakamura M, Ishida E, Shimada K, Kishi M, Nakase H, Sakaki T, Konishi N. Frequent LOH on 22q12.3 and TIMP-3 inactivation occur in the progression to secondary glioblastomas. Lab Invest. 2005;85:165-175.

Nduom EK, Hadjipanayis CG, Van Meir EG. Glioblastoma cancer stem-like cells: implications for pathogenesis and treatment. Cancer J. 2012;18:100-6. Review

Nieder C, Grosu AL, Molls M. A comparison of treatment results for recurrent malignant gliomas. Cancer Treat Rev. 2000;26:397-409. Review.

Ogawa C, Kihara A, Gokoh M, Igarashi Y. Identification and characterization of a novel human sphingosine-1-phosphate phosphohydrolase, hSPP2. J Biol Chem. 2003;278:1268–1272.

Ogura R, Tsukamoto Y, Natsumeda M, Isogawa M, Aoki H, Kobayashi T, YoshidaS, Okamoto K, Takahashi H, Fujii Y, Kakita A. Immunohistochemical profiles of IDH1, MGMT and P53: Practical significance for prognostication of patients with diffuse gliomas. Neuropathology. 2015;35:324-335.

Ohgaki H, Kleihues P. Genetic pathways to primary and secondary glioblastoma. Am J Pathol. 2007;170:1445-53. Review.

Ohgaki H, Kleihues P. Population-based studies on incidence, survival rates, and genetic alterations in astrocytic and oligodendroglial gliomas. J Neuropathol Exp Neurol. 2005;64:479-89. Review.

Oliver TG, Wechsler-Reya RJ. Getting at the root and stem of brain tumors. Neuron. 2004;42:885–888.

Park JW, Park WJ, Futerman AH. Ceramide synthases as potential targets for therapeutic intervention in human diseases. Biochim Biophys Acta. 2013;1841:671–681.

Payne SG, Milstien S, Spiegel S. Sphingosine-1-phosphate: dual messenger functions. FEBS Lett. 2002;531:54-7. Review

Pegg AE. Repair of O(6)-alkylguanine by alkyltransferases. Mutat Res. 2000;462:83-100. Review.

Persano L, Rampazzo E, Basso G, Viola G. Glioblastoma cancer stem cells: Role of the microenvironment and therapeutic targeting. Biochem Pharmacol. 2013;85:612–622.

Plate KH, Scholz A, Dumont DJ. Tumor angiogenesis and anti-angiogenic therapy in malignant gliomas revisited. Acta Neuropathol. 2012;124:763-775.

Pojo M, Costa BM. Molecular hallmarks of gliomas. In: Garami M, editor. Molecular targets of CNS tumors. Rijeka: InTech. 2011:pp 177–200.

Quint K, Stiel N, Neureiter D, Schlicker HU, Nimsky C, Ocker M, Strik H, Kolodziej MA. The role of sphingosine kinase isoforms and receptors S1P1, S1P2, S1P3, and S1P5 in primary, secondary, and recurrent glioblastomas. Tumour Biol. 2014;35:8979–8989.

Reardon DA, Wen PY, Desjardins A, Batchelor TT, Vredenburgh JJ. Glioblastoma multiforme: an emerging paradigm of anti-VEGF therapy. Expert Opin Biol Ther. 2008;8:541–553.

Reya T, Morrison SJ, Clarke MF, Weissman IL. Stem cells, cancer and cancer stem cells. Nature. 2001;414:105–111.

Riboni L, Viani P, Bassi R, Stabilini A, Tettamanti G. Biomodulatory role of ceramide in basic fibroblast growth-factor induced proliferation of cerebellar astrocytes in primary culture. Glia. 2000;32:137–145.

Riboni L, Campanella R, Bassi R, Villani R, Gaini SM, Martinelli-Boneschi F, Viani P, Tettamanti G. Ceramide levels are inversely associated with malignant progression of human glial tumors. Glia. 2002;39:105–113.

.

Riccitelli E, Giussani P, di Vito C, Condomitti G, Tringali C, Caroli M, Galli R, Viani P, Riboni L. Extracellular sphingosine-1-phosphate: A novel actor in human glioblastoma stem cell survival. PLoS One. 2013;8:e68229;

Rich JN, Bigner DD. Development of novel targeted therapies in the treatment of malignant glioma. Nat Rev Drug Discov. 2004;3:430-46. Review.

Rosen H, Goetzl EJ. Sphingosine-1-phosphate and its receptors: An autocrine and paracrine network. Nat Rev Immunol. 2005;5:560–570.

Sakariassen PO, Prestegarden L, Wang J, et al. Angiogenesis-independent tumor growth mediated by stem-like cancer cells. Proc Natl Acad Sci U S A. 2006;103:16466–16473.

Salmaggi A, Boiardi A, Gelati M, Russo A, Calatozzolo C, Ciusani E, Sciacca FL, Ottolina A, Parati EA, La Porta C, Alessandri G, Marras C, Croci D, De Rossi M. Glioblastoma-derived tumorospheres identify a population of tumor stem-like cells with angiogenic potential and enhanced multidrug resistance phenotype. Glia. 2006;54:850–860.

Schmidt KF, Ziu M, Schmidt NO, Vaghasia P, Cargioli TG, Doshi S, Albert MS, Black PM, Carroll RS, Sun Y. Volume reconstruction techniques improve the correlation between histological and in vivo tumor volume measurements in mouse models of human gliomas. J Neurooncol. 2004;8:207–215.

Serwer LP, James CD. Challenges in drug delivery to tumors of the central nervous system: an overview of pharmacological and surgical considerations. Adv Drug Deliv Rev. 2012;64:590–597.

Shu X, Wu W, Mosteller RD, Broek D. Sphingosine kinase mediates vascular endothelial growth factor-induced activation of ras and mitogen-activated protein kinases. Mol Cell Biol 2002;22:7758–7768.

Siegel R, Ward E, Brawley O, Jemal A. Cancer statistics, 2011: the impact of eliminating socioeconomic and racial disparities on premature cancer deaths. CA Cancer J Clin. 2011;61:212e36

Singh SK, Clarke ID, Terasaki M, Bonn VE, Hawkins C, Squire J, Dirks PB. Identification of a cancer stem cell in human brain tumors. Cancer Res. 2003;63:5821–5828

Singh SK, Hawkins C, Clarke ID, Squire JA, Bayani J, Hide T, Henkelman RM, Cusimano MD, Dirks PB. Identification of human brain tumour initiating cells. Nature. 2004;432:396-401.

Son MJ, Woolard K, Nam DH, Lee J, Fine HA. SSEA-1 is an enrichment marker for tumor-initiating cells in human glioblastoma. Cell Stem Cell. United States. 2009; pp. 440-452

Spiegel S, Merrill AH Jr. Sphingolipid metabolism and cell growth regulation. FASEB J. 1996; 10:1388–1397.

Steck PA, Ligon AH, Cheong P, Yung WK, Pershouse MA. Two tumor suppressive loci on chromosome 10 involved in human glioblastomas. Genes Chromosomes Cancer. 1995;12:255–261.

Stewart LA. Chemotherapy in adult high-grade glioma: a systematic review and meta-analysis of individual patient data from 12 randomised trials. Lancet. 2002;359:1011-8. Review.

Stummer W, Pichlmeier U, Meinel T, Wiestler OD, Zanella F, Reulen HJ; ALA-Glioma Study Group. Fluorescence-guided surgery with 5-aminolevulinic acid for resection of malignant glioma: a randomised controlled multicentre phase III trial. Lancet Oncol. 2006;7:392-401.

Stupp R, Roila F; ESMO Guidelines Working Group. Malignant glioma: ESMO clinical recommendations for diagnosis, treatment and follow-up. Ann Oncol. 2008;19(2):ii83-5.

Stupp R, Mason WP, van den Bent MJ, Weller M, Fisher B, Taphoorn MJ, Belanger K, Brandes AA, Marosi C, Bogdahn U, Curschmann J, Janzer RC, Ludwin SK, Gorlia T, Allgeier A, Lacombe D, Cairncross JG, Eisenhauer E, Mirimanoff RO; European Organisation for Research and Treatment of Cancer Brain Tumor and Radiotherapy Groups; National Cancer Institute of Canada Clinical Trials Group. Radiotherapy plus concomitant and adjuvant temozolomide for glioblastoma. N Engl J Med. 2005;352:987-996.

Sullards MC, Wang E, Peng Q, Merrill AH Jr. Metabolomic profiling of sphingolipids in human glioma cell lines by liquid chromatography tandem mass spectrometry. Cell Mol Biol (Noisy-le-Grand). 2003;49:789–797.

Suzuki H, Murasaki K, Kodama K, Takayama H. Intracellular localization of glycoprotein VI in human platelets and its surface expression upon activation. Br J Haematol. 2003;121:904-912.

Terés S, Lladó V, Higuera M, Barceló-Coblijn G, Martin ML, Noguera-Salvà MA, Marcilla-Etxenike A, García-Verdugo JM, Soriano-Navarro M, Saus C, Gómez-Pinedo U, Busquets X, Escribá PV. 2-Hydroxyoleate, a nontoxic membrane binding anticancer drug, induces glioma cell differentiation and autophagy. Proc Natl Acad Sci U S A 2012;109:8489–8494.

Van Brocklyn J, Letterle C, Snyder P, Prior T. Sphingosine-1-phosphate stimulates human glioma cell proliferation through Gi-coupled receptors: Role of ERK/MAP kinase and phosphatidylinositol 3-kinase b. Cancer Lett. 2002;181:195–204.

Van Brocklyn JR, Jackson CA, Pearl DK, Kotur MS, Snyder PJ, Prior TW. Sphingosine kinase-1 expression correlates with poor survival of patients with glioblastoma multiforme: roles of sphingosine kinase isoforms in growth of glioblastoma cell lines. J Neuropathol Exp Neurol. 2005;64:695-705.

van den Bent MJ, Dubbink HJ, Marie Y, et al. IDH1 and IDH2 mutations are prognostic but not predictive for outcome in anaplastic oligodendroglial tumors: a report of the European Organization for Research and Treatment of Cancer Brain Tumor Group. Clin Cancer Res 2010;16:1597-1604.

van den Bent MJ, Dubbink HJ, Sanson M et al. MGMT promoter methylation is prognostic but not predictive for outcome to adjuvant PCV chemotherapy in anaplastic oligodendroglial tumors: a report from EORTC Brain Tumor Group Study 26851. J Clin Oncol 2009;27: 5881-5886.

Verhaak RG, Hoadley KA, Purdom E, Wang V, Qi Y, Wilkerson MD, Miller CR, Ding L, Golub T, Mesirov JP, Alexe G, Lawrence M, O'Kelly M, Tamayo P, Weir BA, Gabriel S, Winckler W, Gupta S, Jakkula L, Feiler HS, Hodgson JG, James CD, Sarkaria JN, Brennan C, Kahn A, Spellman PT, Wilson RK, Speed TP, Gray JW, Meyerson M, Getz G, Perou CM, Hayes DN; Cancer Genome Atlas Research Network. Integrated genomic analysis identifies clinically relevant subtypes of glioblastoma characterized by abnormalities in PDGFRA, IDH1, EGFR, and NF1. Cancer Cell. 2010;17:98-110.

Viani P, Giussani P, Brioschi L, Bassi R, Anelli V, Tettamanti G, Riboni L. Ceramide in nitric oxide inhibition of glial cell growth. P J Biol Chem 2003;278:9592-9601

von Deimling A, Korshunov A, Hartmann C. The next generation of glioma biomarkers: MGMT methylation, BRAF fusions and IDH1 mutations. Brain Pathol. 2011;21:74-87.

Walid MS. Prognostic factors for long-term survival after glioblastoma. Perm J. 2008 Fall;12:45-48.

Walker MD, Alexander E Jr, Hunt WE, MacCarty CS, Mahaley MS Jr, Mealey J Jr, Norrell HA, Owens G, Ransohoff J, Wilson CB, Gehan EA, Strike TA. Evaluation of BCNU and/or radiotherapy in the treatment of anaplastic gliomas. A cooperative clinical trial. J Neurosurg. 1978;49:333-343.

Wang J, Sakariassen PØ, Tsinkalovsky O, Immervoll H, Bøe SO, Svendsen A,

Prestegarden L, Røsland G, Thorsen F, Stuhr L, Molven A, Bjerkvig R, Enger PØ. CD133 negative glioma cells form tumors in nude rats and give rise to CD133 positive cells. Int J Cancer. 2008;122:761–768

Weller M, van den Bent M, Hopkins K, Tonn JC, Stupp R, Falini A, Cohen-Jonathan-Moyal E, Frappaz D, Henriksson R, Balana C, Chinot O, Ram Z, Reifenberger G, Soffietti R, Wick W; European Association for Neuro-Oncology (EANO) Task Force on Malignant Glioma. EANO guideline for the diagnosis and treatment of anaplastic gliomas and glioblastoma. Lancet Oncol. 2014;15:e395-403.

Wen PY, Kesari S. Malignant gliomas in adults. N Engl J Med. 2008;359:492-507.

Wernicke AG, Edgar MA, Lavi E, Liu H, Salerno P, Bander NH, Gutin PH. Prostate-specific membrane antigen as a potential novel vascular target for treatment of glioblastoma multiforme. Arch Pathol Lab Med. 2011;135:1486-1489.

Wick W, Meisner C, Hentschel B, Platten M, Schilling A, Wiestler B, Sabel MC, Koeppen S, Ketter R, Weiler M, Tabatabai G, von Deimling A, Gramatzki

D, Westphal M, Schackert G, Loeffler M, Simon M, Reifenberger G, Weller M. Prognostic or predictive value of MGMT promoter methylation in gliomas depends on IDH1 mutation. Neurology. 2013;81:1515-1522.

Woo SR, Oh YT, An JY, Kang BG, Nam DH, Joo KM. Glioblastoma specific antigens, GD2 and CD90, are not involved in cancer stemness. Anat Cell Biol. 2015;48:44-53.

Yan H, Parsons DW, Jin G, McLendon R, Rasheed BA, Yuan W, Kos I, Batinic-Haberle I, Jones S, Riggins GJ, Friedman H, Friedman A, Reardon D, Herndon J, Kinzler KW, Velculescu VE, Vogelstein B, Bigner DD. IDH1 and IDH2 mutations in gliomas. N Engl J Med. 2009;360:765-773.

Yester JW, Tizazu E, Harikumar KB, Kordula T. Extracellular and intracellular sphingosine-1-phosphate in cancer. Cancer Metastasis Rev 2011;30:577–597.

Yoshida Y, Nakada M, Harada T, Tanaka S, Furuta T, Hayashi Y, Kita D, Uchiyama N, Hayashi Y, Hamada J. sphate receptor type 1 is related to MIB-1 labeling index and predicts survival of glioblastoma patients. J Neurooncol. 2010;98:41–47.

Yoshida Y, Nakada M, Sugimoto N, Harada T, Hayashi Y, Kita D, Uchiyama N, Hayashi Y, Yachie A, Takuwa Y, Hamada J. Sphingosine-1-phosphate receptor type 1 regulates glioma cell proliferation and correlates with patient survival. Int J Cancer. 2010;126:2341–2352.

Zeppernick F, Ahmadi R, Campos B, Dictus C, Helmke BM, Becker N, Lichter P, Unterberg A, Radlwimmer B, Herold-Mende CC. Stem cell marker CD133 affects clinical outcome in glioma patients. Clin Cancer Res 2008;14:123–129.

Zhang J, Hummersone M, Matthews CS, Stevens MF, Bradshaw TD. N3-substituted temozolomide analogs overcome methylguanine-DNA methyltransferase and mismatch repair precipitating apoptotic and autophagic cancer cell death. Oncology. 2015;88:28-48.

Zhang M, Song T, Yang L, Chen R, Wu L, Yang Z, Fang J. Nestin and CD133: valuable stem cell-specific markers for determining clinical outcome of glioma patients. J Exp Clin Cancer Res. 2008; 27: 85

Zhang H, Li W, Sun S, Yu S, Zhang M, Zou F. Inhibition of sphingosine kinase 1 suppresses proliferation of glioma cells under hypoxia by attenuating activity of extracellular signal-regulated kinase. Cell Prolif. 2012;45:167–175.

Ziche M, Morbidelli L, Choudhuri R, Zhang HT, Donnini S, Granger HJ, Bicknell R. Nitric oxide synthase lies downstream from vascular endothelial growth factor-induced but not basic fibroblast growth factor-induced angiogenesis. J Clin Invest. 1997;99:2625-34.